Microbial Sulfur Biogeochemistry of Oil Sand Composite Tailings with Depth

Microbial S Biogeochemistry of Oil Sand Composite Tailings with Depth

By

Kathryn Elizabeth Kendra, B.Sc. (Hons)

A Thesis

Submitted to the School of Graduate Studies

In Partial Fulfillment of the Requirements

For the Degree

Master of Science

McMaster University

Master of Science (2013)	McMaster University
(Geography and Earth Sciences)	Hamilton, Ontario

Title:	Microbial Sulfur Biogeochemistry of Oil Sands Composite Tailings with Depth
Author:	Kathryn E. Kendra, B.Sc. (Honours) (McMaster University)
Supervisor:	Dr. Lesley A. Warren
Number of Pages:	x, 72

Abstract

Surface mining of Alberta's oil sands has led to significant land disturbance, making reclamation and sustainable development of this resource one of the largest challenges facing the industry today. Syncrude Canada Ltd. has developed an innovative technique to reclaim composite tailings (CT) through constructed wetland landscapes and is currently investigating the viability of a pilot-scale freshwater fen built over sandcapped CT. Unpredicted by abiotic geochemical modelling of CT behaviour, a minor episode of hydrogen sulfide (H_2S) gas release was encountered during the initial stages of fen construction indicating microbial activity was likely involved in H_2S generation within CT. This thesis investigates the S geochemistry of CT with depth and employed 454 pyrosequencing and functional enrichments to characterize the associated microbial communities in the first S biogeochemical study of oil sands CT. Porewater H_2S was detected extensively throughout the deposit with background levels ranging from 14 – 23 µM and a maximum of 301.5 µM detected at 22-24 m of depth. Reduced Fe (Fe^{2+}) was also detected, but confined within surficial depths sampled, ranging from 1.2 – 38.5 µM. Mass balance calculations identify that the Fe^{2+} generated within the surficial zone of the CT deposit is sufficient to effectively sequester ambient concentrations H_2S generated in this deposit through FeS precipitates. Results identifying (1) distinct zones of porewater Fe^{2+} and H_2S, (2) co-occurrence of the highest [H_2S] and lowest dissolved organic C (DOC) at 22-24 m consistent with heterotrophic sulfate reducing bacteria (SRB) activity, and (3) the presence of mixed valence Fe biomineral, magnetite, throughout the deposit, are all consistent with microbially-mediated Fe and S cycling occurring within this CT deposit. The cultivation independent identification of several known iron reducing bacteria (IRB) and SRB within CT microbial communities, in conjunction with observed positive growth of IRB and SRB functional

metabolic enrichments, demonstrates widespread capacity for microbial Fe and S activity throughout the CT deposit. Metagenomic characterization of CT microbial communities revealed high diversity (over 20 phyla) over the 5 depths examined. Multivariate statistical analyses (Unifrac) revealed that bacterial community composition and structure was driven by changed in DOC, ORP and salinity and that structuring corresponded with a surficial zone of Fe^{3+} reduction and an underlying zone of SO_4^{2-} reduction. Despite the high organic carbon (OC) content of oil sands tailings, much of that C is not considered to be labile and accessible to microbes. Based on the results of this thesis, CT SRB appear to have a greater ability than IRB to utilize recalcitrant OC (e.g. bitumen, naphthenic acids) given the widespread occurrence of porewater [H_2S] and surficially restricted [Fe^{2+}] despite accessible pools of Fe^{3+} and OC with depth. This enhanced understanding of biogeochemical S cycling within CT newly establishes the importance of microbial activity in these processes, identifying the need to incorporate microbially based understanding into on-going development of reclamation strategies in order to manage these waste materials effectively.

Acknowledgements

I would like to express my sincere gratitude to my supervisor Dr. Lesley Warren for continuous support and encouragement throughout my M.Sc. study and research. Thank you for your wisdom, patience, motivation and uncanny knack of knowing exactly how much I am capable of.

I wish to thank my committee members, Dr. Greg Slater and Dr. Jim Smith, and my chair, Dr. Antonio Paez, for their time inputs, constructive comments and feedback which helped to enhance the effectiveness of this thesis.

I thank my fellow labmates of the Aquatic and Microbial Geochemistry Research Lab group for your support, insightful discussions and all the fun times we have had over the past two years. Specifically, I would like to thank Tara Colenbrander, Steve Holland, Kate Stephenson, Michelle Reid and Derek Amores for field assistance, experimental planning and set up and general lab guidance, and Talitha Santini and Amy Elliott for their metagenomic expertise. I wish to extend my thanks to Robert Donahue and Tara Penner with the Syncrude Mildred Lake Environmental Research group and Wen He Gong at McMaster University for his assistance with XRD analysis.

I would like to acknowledge my wonderful family and friends for continuous support, love and encouragement throughout my thesis writing experience. Thank you for the hilarious pep talks and editing assistance!

In conclusion, I gratefully recognize the Natural Sciences and Engineering Research Council of Canada via an NSERC DG to L.A.W. and Syncrude Canada Ltd. for funding this research.

Table of Contents

List of Figures

List of Tables

INTRODUCTION

Sulfur (S) is a naturally occurring, abundant (~0.05% abundance) element that is widespread throughout the Earth's crust and essential for life (i.e. metabolism, proteins); thus S is a key component in global biogeochemical cycling. Because of its capability to exist in multiple oxidation states ranging from S(-II) to S(+VI), S participates in redox reactions, supporting a wide array of microbial S-based metabolisms. S cycling is driven by combined biological and abiotic processes and system parameters including pH, temperature, redox status, salinity and other ionic constituents that may be present in the system (Bernier, 2007; Wu, et al., 2013). In addition, S dynamics are tightly coupled with and largely affected by Fe dynamics. As such, both abiotic and microbially-mediated S dynamics have been extensively studied in an effort to gain a more comprehensive understanding of how this cycle operates in each unique environment. S dynamics are important and are of interest in a variety of environmental systems, ranging from natural wetland, groundwater, oceanic and lacustrine systems, to anthropogenically-impacted contexts (e.g. acid mine drainage (AMD) and acid sulphate soils) (Burton, et al., 2011a; Wu, et al., 2013). With recent advancements in geochemical analytical capabilities, in conjunction with enhanced understanding of S geochemistry, it has become increasingly evident that S interactions are more complicated and diverse than previously appreciated. It is necessary to explore S dynamics and the associated biogeochemistry throughout a broad range of environments to gain insight as to the role of S and its influence on geochemical evolution in new and emerging S-rich environments (e.g. oil sands mine tailings).

Sulfur can exist in multiple oxidative states ranging from sulfide (e.g. S^{2-}) to sulfate (S^{6+} as SO_4^{2-}), and can exist as a number of aqueous, gaseous and solid species; changes in S speciation

are often tightly coupled to redox-driven biological and abiotic reaction pathways. S exists as a wide range of sulfur oxidation intermediates (SOI) with oxidation states ranging from –I to +V (e.g. elemental S (S^0), thiosulfate ($S_2O_3^{2-}$), sulfite (SO_2^{3-}) and polysulfides (e.g. S_n^{2-} or HS_n^{2-}) as well as organic forms (e.g. thiols) (Hazeu, et al., 1988; Bernier, 2007; Wu, et al., 2013). Given that S can exhibit a diverse array of oxidation states, there is the potential for diverse abiotic and microbially-driven redox processes (Figure 1.1).

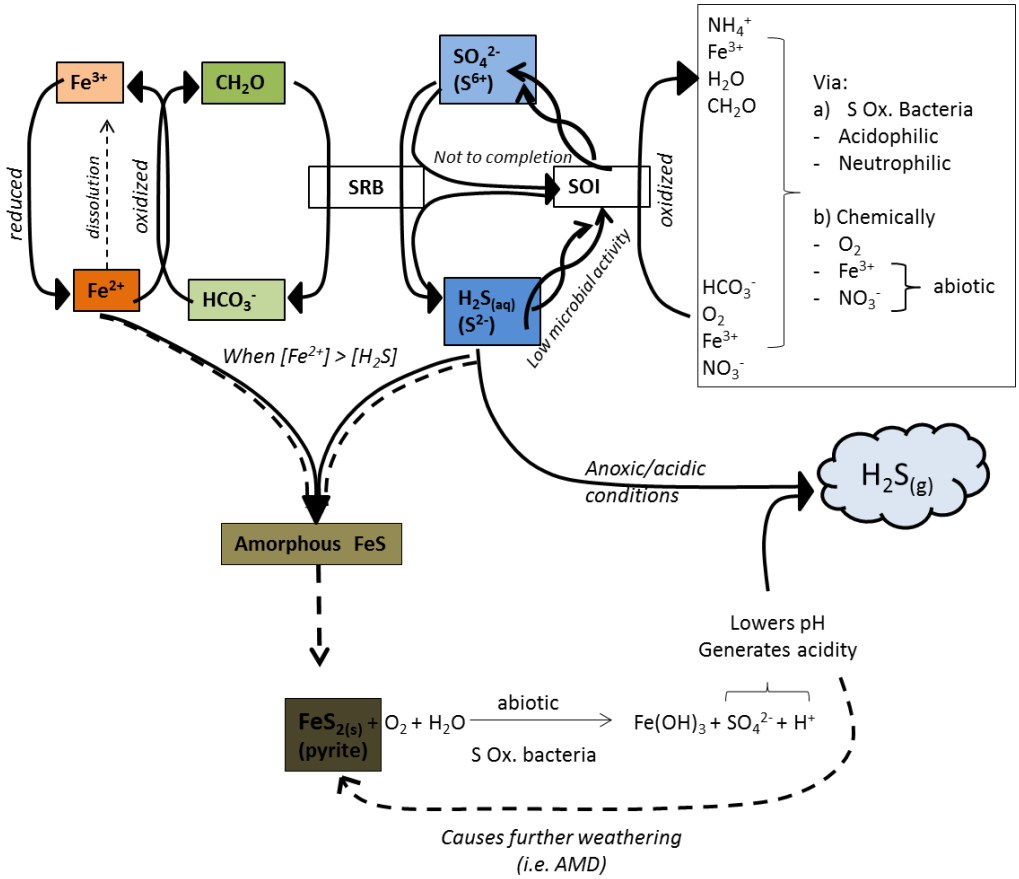

Figure 0.1. Components of the S cycle driven by sulfate reducing bacteria (SRB) and sulfur oxidizing bacteria (SOB) with intermediate formation of sulfur oxidation intermediates (SOI). The S cycle is tightly coupled with the Fe cycle as illustrated through formation of Fe-sulfide precipitates and H_2S gas build up in the absence of Fe^{2+}.

The progression of terminal electron acceptors (Figure 1.2) preferentially utilized upon oxygen exhaustion in a system is dictated by the thermodynamic energy yield an organism can obtain from that reaction in accordance with the redox ladder (Middelburg & Levin, 2009). Despite the relatively low energy yielded from catalysis of redox transformations of S, S-based metabolisms are thought to have been among the earliest to occur on Earth and are still active today (Bernier, 2007). Microorganisms play a key role in the S cycle, affecting the fate of many S species in aquatic environments; however, many of these microbially catalyzed processes are not well constrained (Bernier, 2007; Wu, et al., 2013). The key metabolic pathways driving the biogeochemical cycling of S are S oxidation (via sulfur oxidizing bacteria, SOB), S reduction (via sulfate reducing bacteria, SRB), and S disproportionation (Bernier, 2007; Wu, et al., 2013). The presence of S-based metabolisms and their distribution in the environment are largely determined by geochemical parameters such as pH, redox, salinity, oxygen saturation and availability of organic carbon (OC) (Wu, et al., 2013). Microbial communities have demonstrated a remarkable ability to adapt when exposed to varying conditions or an extreme habitat; for instance microbial communities at Iron Mountain were able to rapidly adjust to AMD and extreme pH conditions (ranging from pH 0.5 to 0.9) and ultimately the community itself changed in response over several years (Druschel, et al., 2004).

1.1 Sulfur Oxidation

Oxidation of reduced S (e.g. sulfide) can occur both abiotically (Equation 1) and biotically (example in Equation 2), depending on the prevailing geochemical conditions. Sulfide will

$$H_2S + 2O_2 \rightarrow {SO_4}^{2-} + 2H^+ \quad (1)$$

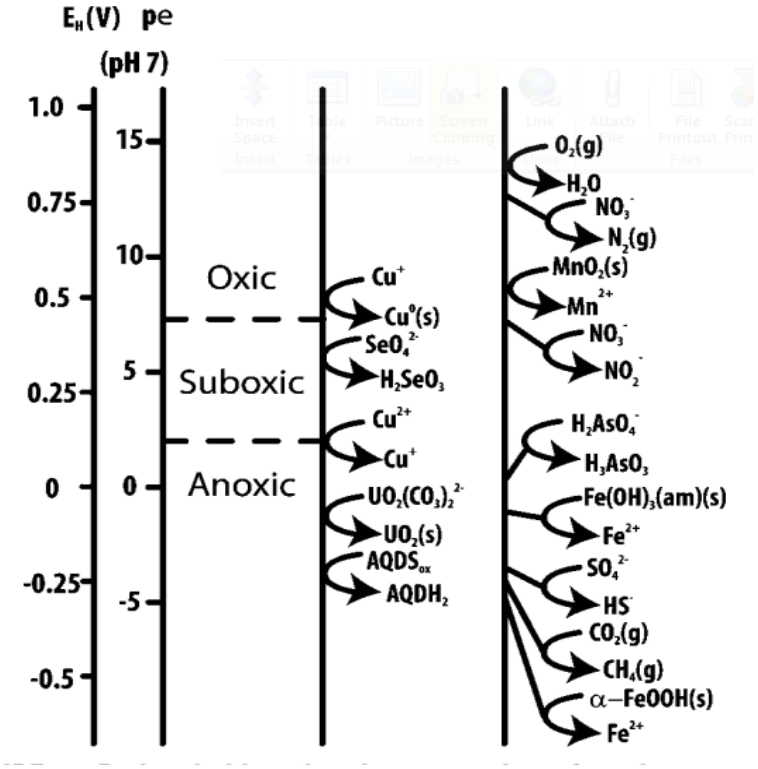

Figure 0.2. The redox ladder of environmentally relevant species and the energy associated with each half reaction (Borch, et al., 2010).

$$NO_3^- + H_2S \rightarrow SO_4^{2-} + NH_4^+ + 2H^+ \quad (2)$$

oxidize rapidly under oxygenated conditions to produce sulfate or an SOI (Eckford & Fedorak, 2002; Zopfi, et al., 2004). Oxidative weathering of pyrite (FeS_2) commonly produces thiosulfate ($S_2O_3^{2-}$) whereas biogenic S oxidation commonly produces S^0 (Druschel, et al., 2004; Bernier, 2007). Due to the rapid abiotic oxidation of sulfide in the presence of oxidants such as O_2, bacteria must develop strategies (e.g. motility) and occupy specific ecological niches (e.g. oxic/anoxic interfaces) in order to effectively compete with abiotic oxidation processes for sulfide (Zopfi, et al., 2004). In addition, S oxidizers tend to complete small, step-wise reactions hypothesized to maximize energy yield, rather than facilitating the complete oxidation of S^{2-} to S^{6+}. For example, H_2S may be oxidized to S^0, which is then later oxidized to sulfite by a different microbe and later completely oxidized to sulfate (Zopfi, et al., 2004). S-oxidizing bacteria are often associated with acidic environments, and are able to drive sulfuric acid generation in AMD environments through oxidation of pyrite and sulfidic minerals (Equations 3 and 4). This strategy allows the bacteria to effectively compete with abiotic oxidation of S^{2-} as potential oxidants (e.g. Fe^{3+}) are able to remain in solution at low pH (< 3). However, this is not always the case as S-oxidizing bacteria have been found in circumneutral environments including anoxic lacustrine and marine sediments, groundwater systems and of specific interest to this thesis, oil sands tailings ponds (Druschel, et al., 2004; Konhauser, 2007; Ramos-Padron, et al., 2011; Golby, et al., 2012). While S-oxidizing bacteria will grow under oxygenated conditions where energy yields are maximized, many S-oxidizing bacteria are also able to grow

in the absence of oxygen using ferric iron (Fe^{3+}) or nitrate (NO_3^-) as the alternate terminal electron acceptors (Bernier, 2007; Burton, et al., 2011a).

1.2 Sulfate Reduction

Bacteria capable of reducing oxidized S species (e.g. SO_4^{2-}, S^0, $S_2O_3^{2-}$, SO_2^{3-}, etc.) are heterotrophic microbes that metabolize primarily under anaerobic conditions (Bernier, 2007; Wu, et al., 2013). Equation 3 and 4 illustrate SO_4^{2-} reduction pathways via sulfate reducing bacteria (SRB) metabolism.

$$SO_4^{2-} + 4H_2 \rightarrow H_2S + 2OH^- + 2H_2O \quad (3)$$

$$CH_3COO^- + SO_4^{2-} + H_2O \rightarrow H_2S + 2HCO_3^- + OH^- \quad (4)$$

Rates of SO_4^{2-} reduction and the subsequent depth of the SO_4^{2-} reducing zone in sediments are generally affected by the conditions of the system such as pH, temperature, types and concentrations of other terminal electron acceptors (i.e. NO_3^-, Fe^{3+}) and OC content. For example, moderate acidity, frequent replenishment of SO_4^{2-} sources, increased temperature and high OC content promote SO_4^{2-} reduction (Mitterer, 2010; Sanz-Lazaro, et al., 2011; Wu, et al., 2013). Hydrogen sulfide, the end product of SO_4^{2-} reduction, may be sequestered through mineral precipitates with divalent cations (e.g. FeS_x, PbS, ZnS) or re-oxidized abiotically (e.g. to S^0 through interactions with O_2, NO_3^- or Fe-(hydr)oxides) (Bernier, 2007; Burton, et al., 2011b; Wu, et al., 2013). Hydrogen sulfide speciates in natural waters between H_2S, HS^- and S^{2-} as a function of pH and temperature (Equations 5 and 6) (Morse, et al., 1987; Rickard & Luther,

2007; Wu, et al., 2013). The collective total concentration of these species is typically referred to as ΣH_2S. Decreased pH increases the relative abundance of the H_2S species which readily equilibrates with the gas phase. Hydrogen sulfide is often of concern in many environments due to its potential toxicity and explosiveness in gas form (Middelburg & Levin, 2009; Wu, et al., 2013).

$$H_2S \rightarrow H^+ + HS^- \qquad pK_{a1} = 6.98 \pm 0.03 \tag{5}$$

$$HS^- \rightarrow H^+ + S^{2-} \qquad pK_{a2} > 14 \tag{6}$$

1.3 Sulfur in the Environment

S dynamics are tightly coupled to the biogeochemical cycling of Fe in environmental systems. H_2S will begin to accumulate in sediment porewaters only after the complete removal of the system's Fe^{2+} content through precipitation (e.g. as Fe^{2+}-sulfides); as such, elevated Fe^{2+} content acts as a buffer to mitigate and control episodes of H_2S gas release (Vlademarsen, et al., 2010). Therefore, when Fe^{2+} concentrations are high enough to strip H_2S out of solution (e.g. x:y for Fe_xS_y precipitates) it is unlikely that H_2S will ever reach concentrations considered to be toxic (Sanz-Lazaro, et al., 2011). In Fe-bearing systems, H_2S has the ability to sequester Fe^{2+} (and other trace elements) through mineral precipitation (Bura-Nakic, et al., 2009). These minerals usually start as amorphous precipitates (FeS), which transition to mackinawite (FeS), greigite (Fe_3S_4) and finally mature to the thermodynamically stable pyrite (FeS_2) or pyrrhotite ($Fe_{1-x}S$ where x = 0 to 0.125) (Bura-Nakic, et al., 2009). Equation 7 illustrates the most common pathway of this mineral formation.

$$Fe^{2+} + HS^- \rightarrow FeS_{(s)} + H^+ \quad (7)$$

While the majority of H_2S produced in a system will react to form Fe-monosulfide precipitates, it is estimated that only 30% of these precipitates will remain permanently sequestered; the remainder is subject to continual recycling within the environment (Sell & Morse, 2006).

Fe dynamics and subsequent S interactions are largely affected by system pH. Under acidic conditions H_2S can accumulate and potentially be released as gaseous H_2S, but accumulation is largely controlled by the availability of Fe^{2+}. Fe^{2+} has been shown to demonstrate enhanced mobility under lower pH (e.g. pH = 6) in comparison to higher pH (e.g. pH = 8) by three to four orders of magnitude (Burton, et al., 2011a), therefore, the more acidic an environment is the more mobile and available Fe^{2+} will be to react with H_2S, thereby supporting the potential for more effective sequestration of H_2S. For example, sulfides present in porewaters have been shown to consist of Fe^{2+}-sulfide complexes, aqueous FeS clusters as well as amorphous Fe-sulfide minerals such as mackinawite and greigite (Keene, et al., 2011).

1.3.1 Acid Mine Drainage

AMD systems provide an ideal system in which to explore the pathways and cycling associated with S as many of the pre-existing geochemical conditions have been well studied and documented (Bernier, 2007). AMD refers to the abiotic and/or microbially-catalyzed generation of sulfuric acid and concomitant liberation of metals which become increasingly soluble under

low-pH conditions. Such drainage is typically characterized by high aqueous concentrations of base metals in solution and low OC content (Edwards, et al., 2000; Druschel, et al., 2004; Sanz-Lazaro, et al., 2011). The high relative abundance of reduced Fe- and S-bearing mineral phases commonly observed in base metal, precious metal, and coal-derived mine waste rock and tailings supports microbial oxidative processes and contributes to the growth of chemolithotrophic S and Fe bacteria (Fortin, et al., 1995; Wakelin, et al., 2012). Bacterial communities in these extreme environments have demonstrated a remarkable ability to adapt and survive in these conditions (Wakelin, et al., 2012). Two of the most dominant microbes known to catalyze Fe and S cycling in AMD contexts, *Acidithiobacillus* spp., a S-oxidizing genus and *Acidiphilium* spp., a chemolithotrophic Fe-oxidizing genus have been widely observed across mining environments (Norlund, et al., 2009). These microbes work together to recycle S which effectively diminishes the amount of S oxidation products produced which would otherwise drive down the pH of the system (Lewis, 2010). This highlights the potentially significant interrelationship between Fe and S cycling with associated environmental impacts. Although a host of chemical processes contribute to AMD, pyrite oxidation is by far the greatest contributor (Equation 8) (Edwards, et al., 2000). The oxidation of sulfide (as FeS_2) to sulfate releases Fe^{2+} into solution and generates acidity. The Fe^{2+} is subsequently oxidized to Fe^{3+} by iron oxidizing bacteria (IOB) (Equation 9) which is stable in solutions where pH < 3, thus Fe^{3+} can further oxidize sulfidic minerals (Equation 10) generating more acid than abiotic processes alone (Equation 11) ((Fortin, et al., 1995; Edwards, et al., 2000; Nordstrom, et al., 2000; Bernier & Warren, 2005).

$$2FeS_{2\,(s)} + 7O_2 + 2H_2O \rightarrow 2Fe^{2+}{}_{(aq)} + 4SO_4{}^{2-}{}_{(aq)} + 4H^{+}{}_{(aq)} \quad (8)$$

$$4Fe^{2+}{}_{(aq)} + O_{2\,(g)} + 4H^{+} \rightarrow 4Fe^{3+}{}_{(aq)} + 2H_2O_{(l)} \quad (9)$$

$$FeS_{2\,(s)} + 14Fe^{3+} + 8H_2O_{(l)} \rightarrow 15Fe^{2+}{}_{(aq)} + 2SO_4{}^{2-}{}_{(aq)} + 16H^{+}{}_{(aq)} \quad (10)$$

$$2FeS_{2\,(s)} + 3.75O_2 + 3.5H_2O_{(l)} \rightarrow Fe(OH)_{3\,(s)} + 2SO_4{}^{2-}{}_{(aq)} + 4H^{+}{}_{(aq)} \quad (11)$$

1.3.2 Marine Environments

In contrast to AMD, marine sediments represent a circumneutral pH and OC rich system reflecting carbonate buffering and high OC inputs (Sanz-Lazaro, et al., 2011). In marine environments, the majority of S exists in its most oxidized state (e.g. sulfate) or in its most reduced state (e.g. sulfide including pyrite, pyrrhotite, etc.) (Zopfi, et al., 2004). In modern oceans, sulfate is the second most abundant anion with relatively high concentrations of approximately 29 mM; the ocean thus represents a significant reservoir of oxidized S (Middelburg & Levin, 2009; Xie, et al., 2012). Due to this large reservoir of SO_4^{2-} in seawater and SO_4^{2-} diffusion into anoxic sediments, SO_4^{2-} reduction is a dominant process within marine sediments; thus sulfide is thought to be a key driver of biogeochemical processes in marine sediments (Canfield, 1989). However, the prevalence of porewater H_2S is largely dictated by the activity of SRB and the availability of reactive Fe^{2+} in the system (Omoregie, et al., 2008; Keene, et al., 2011). Fe^{2+}-driven H_2S 'buffering' plays a significant role in marine H_2S accumulation; in Fe^{2+}-rich systems the majority of H_2S (up to 63%) was sequestered through Fe^{2+} precipitates (Vlademarsen, et al., 2010). A study by Sell and Morse (2006) investigated the role of S and Fe pools in marine sediments and observed significant variability across sites in response to chemostratification (e.g. due to salinity), supporting the importance of salinity in influencing S

dynamics. Additionally, the biogeochemistry of marine sediments is perhaps more variable than previously thought as zones of sulfate reduction have been observed to overlap with zones of methanogenesis, depending on the amounts of available OC, sulfate regeneration and sedimentation rates (Oremland, et al., 1982; Mitterer, 2010). While SRB are major contributors to organic matter degradation, further work is still needed to understand the controls and mechanisms of S reduction in organically enriched sediments such as those in marine environments (Vlademarsen, et al., 2010).

1.4 Sulfur Biogeochemistry in the Athabasca Oil Sands

The Athabasca Oil Sands constitute the world's third largest reserves of crude oil and are located within a 140, 200 km^2 bitumen belt in northern Alberta, Canada (Syncrude Canada Ltd, 2010). Demands for unconventional methods of oil recovery have increased in recent years due to the increased global demand for oil. As such, production in Alberta's oil sands has increased greatly, with production reaching approximately 90 million barrels of oil per day (Syncrude Canada Ltd, 2010). Mining companies are responsible for their waste products for which the Canadian government has set strict standards regarding tailing pond expansions and reclamation requirements long past mine closure (Bordenave, et al., 2010; Dimitriu, et al., 2010). As such, there is a definite need for innovative, sustainable and long-term reclamation and tailing management solutions. Syncrude Canada Ltd. has developed a unique strategy by which composite tailings (CT) are utilized to in-fill exhausted open-cast mine pits sites in order to create a base for future reclamation landscapes (SyncrudeCanadaLtd, 2010). CT is a mixture of ~ 18% fluid fine tailings (i.e. saline water, suspended Fe^{3+} rich clay minerals and residual

bitumen) and ~ 82% post-processed sand that has been amended with gypsum ($CaSO_4 \bullet 2H_2O$) which acts as a densifying agent, neutralizing the net negativity of clay minerals to encourage flocculation; the result is a slightly alkaline (pH = 8), moderately saline material with increased trafficability which acts as a base upon which to build reclamation landscapes (Syncrude Canada Ltd, 2010; Ramos-Padron, et al., 2011; Voordouw, 2012).

Recent research has provided evidence of increasing S emissions from the oil sands region, which suggests generation of H_2S within tailings ponds and/or in-filled deposits (i.e. CT) (Proemse, et al., 2012). As discussed, S dynamics demonstrate significant variability in response to prevailing geochemical conditions. Based on the characteristics of CT, it seems likely that the S dynamics of CT resulting in H_2S, will proceed via reaction processes characteristic of marine environments. Like marine sediments, CT is saline, alkaline, has high OC content (residual bitumen) and is largely anoxic. However, like base metal mining contexts there are acidic components to oil sands wastes (i.e. naphthenic acids, NA) which may promote acidophilic microzones within the bulk CT materials. While the microbial ecology of oil sand environments is still not well understood, these environments have been found to host a vast array of microbes including SRB, nitrate reducing bacteria, Fe-reducing bacteria, methanogens, fermenters and acetogens (Dimitriu, et al., 2010; Harner, et al., 2011) as well as acidophilic Fe and S metabolising organisms (Stephenson, 2012). Microbes native to oil sand-associated systems have also been found in marine and freshwater environments (Harner, et al., 2011). These microbes drive many processes and typically result in the generation of methane, sulfide and carbon dioxide (Harner, et al., 2011). Thus an understanding of S and associated Fe dynamics of an oil sands CT deposit, will likely share similarities in Fe and S dynamics from a variety of environmental systems.

Typically, oil sands tailings may contain up to 7% of bitumen residuals (Bordenave, et al., 2010). As such, this residual hydrocarbon material may then act as an OC source to fuel microbial metabolisms, in particular sulfate reduction, leading to established microbial communities within these environments (Fukui, et al., 1999; Hasinger, et al., 2012). In contrast, exposure to crude oil and residual naphthenic acids, both generally considered to be toxic, may have an overall negative effect on microbial communities and cell counts, so much so that in many marine environments, hydrocarbon spills have led to severe ecological damage (Suarez-Suarez, et al., 2011). However, it was found that the introduction of these contaminants can actually enhance rates of sulfate reduction under certain conditions, indicating that SRB may thrive by using hydrocarbons as an energy and OC source; however the exact mechanisms associated with this SRB stimulation were not identified (Suarez-Suarez, et al., 2011; Hasinger, et al., 2012). Additionally, the amendment of gypsum-derived sulfate to CT may further stimulate SRB within the system (Harner, et al., 2011). This suggests that, as in marine sediments, SO_4^{2-} reduction may be a dominant process in a CT deposit leading to potential sulfide formation and release (Schippers & Jorgensen, 2001).

It is important to understand the biogeochemistry of CT in order to understand how a CT deposit will react to varying environmental stimuli. For example, acid sulfate soils (undisturbed pH ~ 7.0) once exposed to oxygen undergo abiotic oxidation of Fe^{2+}-sulfide minerals, which releases Fe^{2+} and S^{2-} into solution and results in acid generation (pH < 4) with severe ecological impacts (Oborn, 1989; Keene, et al., 2011; Nystrand & Osterholm, 2013). Thus, if the pH of CT (pH ~ 8) was to decrease considerably (i.e. high acid generation associated with acidophilic microniches and exhaustion of acid neutralizing capacity (ANC) buffering, anthropogenic additions to the system, land disturbance resulting in oxygenation, etc.) there would be the

potential for sequestered S^{2-} to become remobilized into the porewaters. An environment must be slightly acidic for appreciable concentrations of H_2S to accumulate; thus the occurrence of appreciable concentrations of H_2S within the bulk ΣH_2S pool in circumneutral pH (i.e. ~7-8.5) CT would either reflect the presence of biologically-induced acidophilic microniches (Bertics & Ziebis, 2010; Wu, et al., 2013) or significant rates of SO_4^{2-} reduction and the lack of subsequent H_2S removal through Fe_xS_y precipitation. In AMD environments, acid generation is a by-product of microbial S oxidative processes; acidophilic pockets within a system could reflect the presence of active S oxidizer communities (Druschel, et al., 2004).

RESEARCH SCOPE

Fe and S are ubiquitous, abundant elements occurring across nearly every environment on Earth, including mining contexts where S is highly concentrated in ore deposits and waste residues. The coupled biogeochemical cycling of Fe and S builds a foundation for environmental quality and is highly variable depending on the environmental context involved. Site-specific microbially and abiotically mediated controls, i.e. occurrence and activity of S and Fe metabolizing bacteria, pH, redox status, temperature, salinity and organic carbon content will collectively influence the nature and extent of S and Fe transformations and thus, environmental outcomes. While much investigation has focused on natural and AMD S rich environments, this is the first study to assess S and Fe biogeochemistry in oil sands composite tailings (CT). Oil sand tailings deposits (e.g. CT, tailings ponds) are important S reservoirs with potential global significance due to their increasing prevalence and are known to contain active and diverse

microbial communities. As evidenced by increasing S emissions from the oil sands, active biogeochemical S cycling within CT is likely. With surface mining of Alberta's oil sands spanning over 4,800 km^2 and accelerated production, these tailings-based landscapes will become increasingly prevalent with significant environmental impacts. An understanding of the biogeochemistry of the CT environment is an essential first step in developing effective remediation and management strategies for long-term reclamation throughout the oil sands, as well as contributing to our fundamental knowledge of S and Fe biogeochemical cycling across a broader context of environments. To date, oil sand tailings remain poorly constrained with respect to S biogeochemistry; thus, this research addresses and important fundamental and applied knowledge gap.

Syncrude Canada Limited has developed an innovative technique for dry reclamation of bitumen extraction waste products, through the formation of composite tailings (CT), a mixture of tailings, post-processed sand and gypsum. Currently, Syncrude is investigating the viability of reclaiming a CT deposit through construction of a pilot-scale freshwater fen overlying sandcapped CT. However, during initial phases of fen construction an isolated incident of H_2S gas release occurred, indicating higher levels of H_2S within the CT than predicted by abiotic geochemical modeling of the deposit S geochemistry. Previous research on the reclamation fen has demonstrated microbial Fe and S cycling capabilities and has suggested that the underlying CT itself may be the source of H_2S (Stephenson, 2012); however no direct examination of the CT materials for microbial and Fe/S geochemical characterization has occurred to date. Thus, this thesis characterizes the depth dependent S biogeochemistry of a CT deposit over 36 m (Kingfisher fen, Syncrude Canada, Mildred Lake, Fort McMurray, AB) that has yet to undergo

reclamation activity to establish if H_2S generation is occurring in these materials, and if so, to constrain the behaviour and variables involved.

2.1 Objectives and Hypotheses

The primary research objectives of this thesis are to:

(1) characterize the solid and porewater S, Fe and OC geochemistry of untreated CT with depth throughout the deposit;
(2) evaluate the microbial community composition and metabolic capabilities over these same depths;
(3) identify microbial-geochemical interactions linked to H_2S generation and sequestration occurring within CT.

In association with these research objectives, four hypotheses were tested:

(1) H_2S will occur within CT porewaters and will reflect environmental geochemical conditions, e.g. [OC], [SO_4^{2-}], pH and ORP;
(2) CT will host microbially diverse communities reflecting the OC, Fe and S sources within these materials;

(3) Fe- and S-metabolising bacteria will occur within the CT deposit and will be specifically associated with zones of [Fe^{2+}] and [H_2S] generation, i.e. non-randomly associated with CT;

(4) biogeochemical characteristics of CT will share similarities with both natural (e.g. marine sediments, peatlands and lacustrine sediments) and anthropogenically-impacted (e.g. AMD and oil sands tailings ponds) S-rich environments.

METHODOLOGY

3.1 Field Sampling

3.1.1 Site Location and Description

All samples for this project were collected from the Kingfisher CT deposit, a subsection in the northwest corner of the East-in-Pit tailings deposit at the Mildred lake mine site of Syncrude Canada Ltd., located approximately 50 km north of Fort McMurray, Alberta, Canada (Figure 3.1). The Kingfisher CT deposit consists of a retired open-pit mine site, ~40 m deep, lined with lean oil sands fill above limestone bedrock (~70 m below the surface) which has been in-filled with inter-bedded CT and tailings sand layers with variable grain sizes. CT was deposited at this site through a series of discharge pipes over the span of several years, such that the oldest CT layers are found at the bottom of the deposit with the most recent CT layers towards the surface. Each batch of CT may vary, thus, this deposit is spatially heterogeneous. Reclamation activity at this site has yet to occur, however the Kingfisher CT deposit is located

directly adjacent to the site of a pilot-scale freshwater fen reclamation project undergoing construction. As such, the Kingfisher CT deposit currently provides an ideal 'pre-reclamation' environment in which to study the geochemical processes occurring within CT prior to any impacts of reclamation activity.

Sample collection was conducted from December 4-8th, 2012 and was facilitated through the use of a Fraste ML track-mounted amphibious drill rig fitted with a sonic drill head. Core tubes had a diameter of 50 mm and a minimum length of 2 m and were fitted with an AquaLock valve that enabled retention of the sample during extraction. Due to the high water content of CT (materials easily liquefy upon disturbance), mechanically induced vibrations through the core tube cause a fine layer of CT to liquefy around the core tube reducing friction and resistance and allowing for sample collection. The location of the sampling site is shown in Figure 3.2 (site location: 57°2'19.19" N, 111°34'35.82" W). The sampling strategy was developed from an initial drill sample collection attempt in the fall of 2011 (data not included here) and is described in detail below.

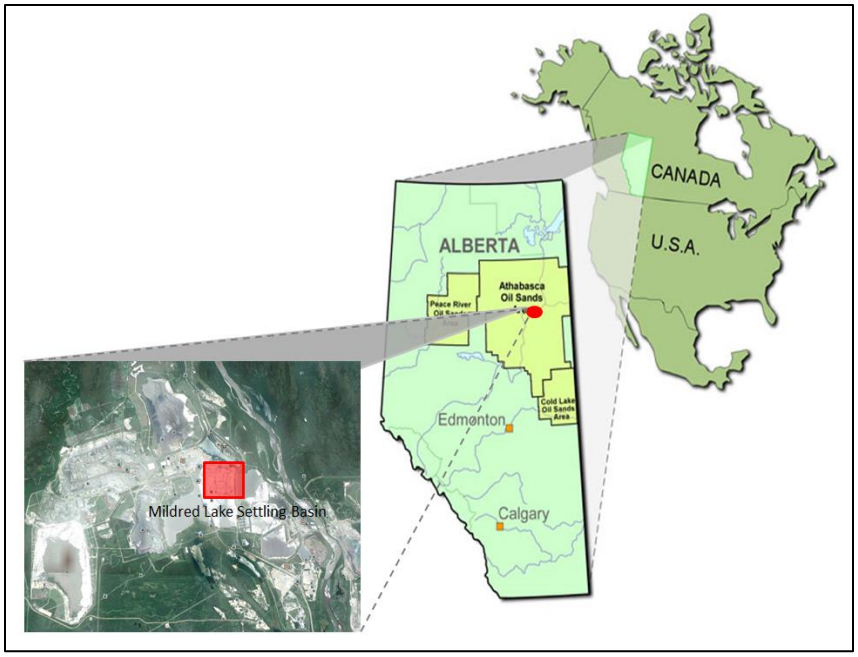

Figure 0.3. The location of the Mildred Lake mine of Syncrude Canada Ltd, located approximately 50 km north of Fort McMurray, Alberta. Images obtained from the Alberta Geological Survey and Google Earth on April 7, 2013.

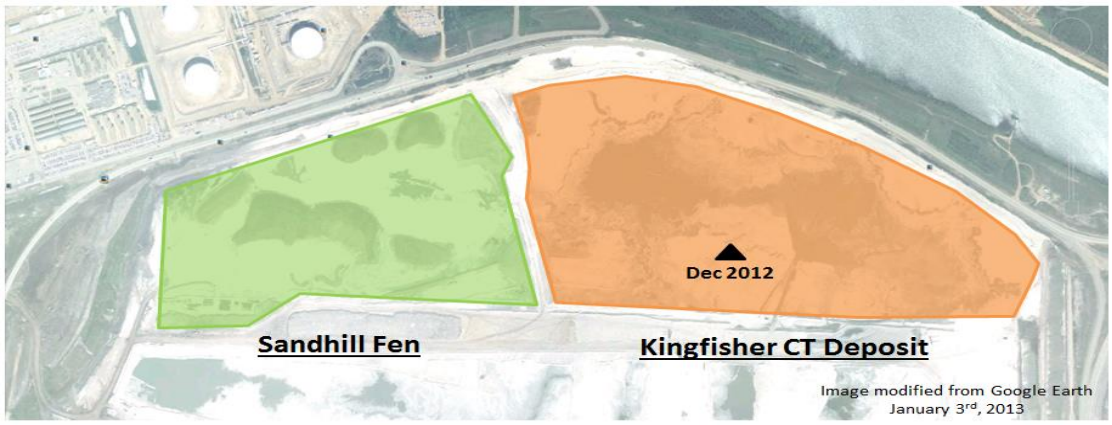

Figure 0.4. The December 2012 drill location within the Kingfisher CT deposit in the East-In-Pit site at Mildred Lake (Syncrude Canada, Fort McMurray AB). Satellite image obtained from Google Earth.

3.1.2 Sample Collection and Analysis

Prior to sample collection for analyses, a complete geochemical depth profile was conducted in which samples were taken at 2 m intervals throughout the CT deposit (0 - 36 m deep) to establish the conditions of the system and determine the depths for sample collection for geochemical and microbiological characterization.

This initial pre-screening of the entire depth of the deposit assessed (a) pH, temperature, conductivity and oxidation reduction potential (ORP) using a YSI Professional Plus handheld probe (YSI Incorporated, Yellow Springs, OH, USA), and (b) the presence of aqueous and/or gaseous H_2S using the following field-level screening tests; (1) detection of aqueous H_2S via a methylene blue colorimetric assessment; (2) lead acetate paper as a colorimetric assessment for H_2S gas; and (3) positive detection of H_2S gas concentrations evolved from a small subsample of CT using an RKI Eagle gas detection unit (Table 3.1). As CT is a highly unconsolidated material, it readily liquefies into a slurry of fine particles (Figure 3.3), thus, it is impossible to generate samples through sectioning of drill core segments. Further, the nature of the drill rig, specifically designed for challenging CT materials, collects drill core material at a minimum depth interval of 2 meters. Thus all 2 m core samples were homogenized prior to sample distribution for various analyses and all analyses here represent a bulk characterization over a 2 m depth interval. All samples were collected in an Atmosbag glove bag (Sigma Aldrich) sealed around the end of the core tube and filled with N_2 gas. All surfaces and instruments were sterilized with 70% ethanol prior to use.

Figure 0.5. Unconsolidated quicksand-like consistency of CT.

Based on the results generated by the initial screening of the entire 36 meters, five depths were selected for in-depth sampling; 2-4 m, 6-8 m, 14-16 m, 22-24 m and 32-34 m where 6-8 m, 14-16 m and 22-24 m tested positive for H_2S and 2-4 m and 32-34 m bracketed evident H_2S zones. Samples were collected for (1) porewater S, Fe and OC characterization, (2) solids mineralogy and Fe/S characterization, (3) microbial community analyses (metagenomic analyses), as well as (4) occurrence of specific functional metabolisms (enrichments). Table 3.2 outlines the samples collected, the collection procedure and the storage details. All samples were taken in 2 m increments and homogenized prior to sample allocation and were preserved until analysis was possible at McMaster University. Approximately 25 mL of CT was aliquoted from the bulk 2 m sample for each environmental enrichments (sterile 50 mL Falcon tube), Fe/S analysis (100 mL Whirlpak bag), XRD (100 mL Whirlpak bag), 16S rRNA sequencing (sterile 15 mL Falcon tube) and TOC/TIC analysis (C-free glass jar). Oxygen sensitive samples (environmental enrichments, Fe/S analysis, XRD) were stored anaerobically in Mylar bags with O_2 absorbing packets (Canadian Survival Company, Ontario, Canada). Samples for Fe/S analysis, XRD,

TOC/TIC and 16S rRNA sequencing were transported and stored at -20ºC until time of analysis while environmental enrichment samples and samples for porewater extraction and analysis were transported and stored at 4ºC until time of analysis. Extraction of porewaters from CT was facilitated through the use of Slide-a-Lyzer cassettes (described in detail below) where CT was extruded into Whirlpak bags and equilibrated with MilliQ water in Slide-a-Lyzer cassettes for 3+ days, at which point waters were then analyzed for H_2S, SO_4^{2-}, Fe^{2+}, Fe^{3+}, DOC and DIC concentrations.

As this is the first study assessing S biogeochemistry of CT materials in the oil sands, an initial field season (Fall 2011) served to develop the sampling protocol for the sample collection in December of 2012 that comprises the results presented in this thesis. During the initial field season, a number of challenges were identified in sampling CT for subsequent analyses. In particular, the separation of porewater from the slurry particulates for analyses was beyond established field protocols of syringe filtering or settlement due to the high proportion of fine clay materials with slow settling times. Indeed, syringe filtering, Whirlpak bags designed for porewater separation and gravity settling all yielded murky water (if any) unsuitable for analysis associated with dissolved porewaters. Thus, a new method was developed for the December 2012 sampling campaign where Slide-a-Lyzer cassettes (Figure 3.4) equipped with dialysis membrane were used to extract porewater (Thermo Scientific). The Slide-a-Lyzers were selected in a 3 mL volume with a 20,000 dalton molecular weight cut off (equivalent to 20,000 g/mol), large enough to allow the compounds of interest (SO_4^{2-}, MW = 96.06 g/mol) to diffuse through. Prior to use in the field, an equilibration experiment was conducted in the laboratory

Table 0.1. Methodological details of the field-level H_2S detection tests used during the geochemical screening of the 36 meter deposit.

Method	Details
Methylene Blue Colorimetric Test (Method 8131, Hach Company)	- 1 mL of Reagent 1 was added to a clean 50 mL polypropylene tube to stabilize any H_2S present - ~5 mL of CT was directly extruded into the tube under anaerobic conditions - total volume was made to 25 mL using distilled H_2O and 1 mL of Reagent 2 was added - tube contents were homogenized and reacted for 5 mins - development of a blue colour indicated the presence of H_2S
Lead Acetate Paper Colorimetric Test	- ~5 - 20 mL of CT was directly extruded into a clean 50 mL polypropylene tube under anaerobic conditions - a strip of lead acetate paper (Sigma Aldrich) was hung over the side of the tube - tubes were tightly sealed and left to sit for ~5 mins - strips turned black in the presence of H_2S gas
Direct Measurement of Evolved Gas	- ~5 - 20 mL of CT was directly extruded into a clean 50 mL polypropylene tube - tubes were tightly sealed and incubated for ~5 mins - tubes were opened on a horizontal angle and the gas detection unit was held at the tube opening to obtain a reading - presence of H_2S gas resulted in positive readings (ppm)

using a known concentration of SO_4^{2-}, whereby Slide-a-Lyzers were filled with degassed MilliQ water and submerged in a mixture of oil sands post-process sand (to mimic diffusion though a

solid) and saturated with a 20 mM solution SO_4^{2-} (using Na_2SO_4, Sigma Aldrich). Water from the submerged Slide-a-Lyzers was sampled at regular intervals (e.g. t = 1, 2, 3, 4, 5 days) and SO_4^{2-} was quantified colorometrically in triplicate using the SulfaVer Hach method (Ultraspec 2000, UV/visible spectrophotometer, Pharmacia Biotech, Cambridge, UK). Equilibration was achieved when the concentration of SO_4^{2-} extracted from the Slide-a-Lyzer was equivalent to the concentration of SO_4^{2-} measured in bulk solution (as the sand contributed SO_4^{2-} to the bulk solution). Equilibration in this experimental time trial was achieved after 3 days. For deployment in the field, Slide-a-Lyzers were filled with degassed MilliQ water in the anaerobic chamber at McMaster University (Forma Scientific, Inc., Marietta, OH, USA) and transported anaerobically to the field site.

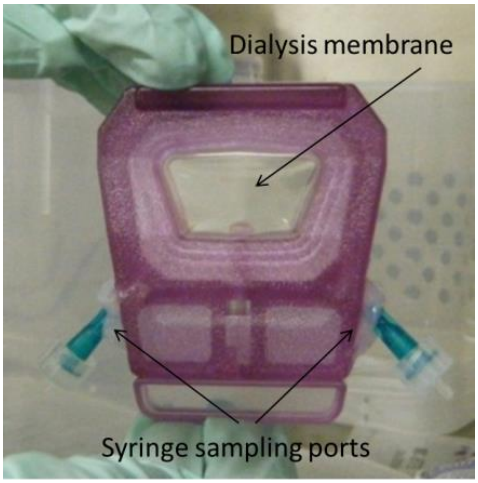

Figure 0.6. Depiction of a Slide-A-Lyzer cassette used for porewater extraction.

Table 0.2. Outline of the samples collected and procedures used for the in-depth sampling conducted on the five select depths.

Sample	Collection	Storage
Environmental Microbial Enrichments	CT was directly extruded into a sterile 50 mL Falcon tube.	Preserved in Mylar bags (Canadian Survival Company, Ontario, Canada) with O_2 absorbing packets at 4°C.
16S rRNA Sequencing	CT was directly extruded into a sterile 15 mL Falcon tube.	Stored on ice for the remainder of the work day until a DNA extraction could be performed (~6-10 hours later).
XRD Analysis	CT was directly extruded into a 15 mL Falcon tube.	Preserved in Mylar bags with O_2 absorbing packets, stored at -20°C until use.
Fe Sequential Extractions & AVS/AES Analysis	CT was aliquoted into a small sterile Whirlpak bag.	Preserved in Mylar bags with O_2 absorbing packets, stored at -20°C until use.
TOC & TIC Analysis	CT was aliquoted into a small C free glass jar.	Stored at -20°C until use.
Porewater Analysis: Fe^{2+}, Fe^{3+} SO_4^{2-},H_2S DOC/DIC	CT was directly extruded into Whirlpak bags containing 6 x 3 mL Slide-a-Lyzer's filled with degassed MilliQ H_2O and equilibrated for 3 - 4 days.	Preserved in Mylar bags with O_2 absorbing packets at 4° C until extraction and analysis in the anaerobic chamber at McMaster University.

3.2 Equilibrium Modelling of H_2S Speciation

Reduced sulfide is a weak acid and speciates between H_2S, HS^- and S^{2-} in the natural environment; this speciation is largely dependent on pH and temperature. Equilibrium modelling

of porewater sulfide species (based on the concentration of $\sum H_2S$ measured in porewaters) was used to determine the portion present as H_2S and thus the portion potentially in exchange with the gas phase. PHREEQC Version 2.18 geochemical modelling software (USGS, available at http://wwwbrr.cr.usgs.gov/projects/GWC_coupled /phreeqc/index.html) was utilized and pH, temperature, ORP, $[Fe^{2+}]$, $[SO_4^{2-}]$ and [inorganic C] were used as input parameters.

3.3 Environmental Microbial Enrichments

Microbial enrichments were utilized to determine whether specific functional metabolic capabilities, i.e. Fe and SO_4^{2-} reduction, existed within the CT materials and to assess the occurrence of these capabilities over the depth of the drill samples. Very few environmental microbes have been identified (< 10%) and of those even less have been cultured (<1%) (Hugenholtz, 2002), thus environmental enrichments (through positive growth) confirm the presence of specific metabolisms within communities. Specific functional metabolisms are enriched from a bulk community by selectively formulating media using the suspected metabolic requirements, energy sources and environmental factors (Burlage et al., 1998). It is important to note that many microbes are capable of more than one type of metabolism and will compete for nutrients so microbial enrichments ultimately demonstrate the metabolic capacity of the system but may not be a true representation of the *in situ* activity. For the purpose of this study, enrichments were made to target SO_4^{2-}-reducing bacteria (SRB), S-oxidizing bacteria (SOB), Fe (III)-reducing bacteria (IRB) and Fe (II)-oxidizing bacteria (IOB).

Preserved sediments were enriched (< 10 days post-sample collection) upon return to the lab after field sampling (preserved anaerobically and stored/transported at 4°C). Enrichments were made by aseptically transferring ~1 g of CT sample into a sterile 50 mL Falcon tube and

supplementing with ~45 mL of media. Aerobic enrichments were made in a Class II A/B3 Biological Safety Cabinet (BSC) (Model 1284, Forma Scientific Inc., Ohio, USA) to ensure sterility while anaerobic enrichments were made in an anaerobic chamber with all surfaces thoroughly sterilized with 70% v/v ethanol prior to beginning. Caps of the Falcon tubes were loosely sealed to encourage gas exchange but limit foreign bacteria from entering the sample. All media was sterilized prior to use by either: (1) autoclaving at 121°C for 30 minutes; or (2) passing through a 0.22µm filter paper using a Nalgene vacuum filter column (Thermo Scientific). Anaerobic media was degassed under N_2 gas flow for 45 minutes and filter sterilized (0.22µm) in the anaerobic chamber. After initial growth, subsequent enrichments were made by combining 5 mL of the original enrichment with 40 mL of fresh media in a sterile 50 mL Falcon tube. Incubation conditions, positive growth indicators and specific media conditions for each metabolism are outlined in the following sections 3.2.1 to 3.2.5.

3.3.1 SO_4^{2-} Reducing Bacteria

Heterotrophic SRB were grown on a lactate media as outlined by Burlage et al. (1998). Media was autoclaved at 121°C for 30 minutes and degassed under N_2 gas flow for 45 minutes. Media was transferred to an anaerobic chamber and filter-sterilized to ensure sterility after degassing. All enrichments were carried out in an anaerobic chamber with all surfaces sterilized with 70% v/v ethanol. Positive growth was indicated by the formation of a black FeS precipitate.

3.3.2 Neutrophilic S-Oxidizing Bacteria

Neutrophilic, chemolithotrophic S oxidizing bacteria were grown on *Thiobacillus aquaesulis* media, using thiosulfate ($S_2O_3^{2-}$) as the electron donor, as outlined by Burlage et al.

(1998). Two to three drops of phenol red pH indicator were added to each enrichment, and the pH was adjusted using sterile NaOH such that the indicator turned pink (pH > 8). Positive growth was indicated by the pH indicator turning yellow (pH < 8), signifying acid generation by S oxidation.

3.3.3 Acidophilic S-Oxidizing Bacteria

Acidophilic, chemolithotrophic S oxidizing bacteria were grown in a modified ATCC 125 media using tetrathionate ($S_4O_6^{2-}$) an electron donor. The following concentrations were achieved in the media: 1.5 mM of $(NH_4)_2SO_4$; 2.1 mM of $MgSO_4 \cdot 7H_2O$; 2.5 mM of $CaCl_2 \cdot 2H_2O$; 3.7 mM of KH_2PO_4; 16.5 mM of $K_2S_4O_6$; and 36 µM of $FeSO_4 \cdot 7H_20$ (Bernier and Warren, 2007). $FeSO_4 \cdot 7H_20$ was added immediately prior to filter sterilization through a 0.22µm filter paper. Upon initial enrichment, 2 - 3 drops of bromothymol blue pH indicator were added to each culture and the pH was adjusted using a bench top pH meter (Denver Instrument Company, Denver, CO, Model 215) with a 3M KCl high-performance pH/ATC glass-body electrode to pH 4 using sterile 1 M KOH or 0.1 N H_2SO_4. The pH meter probe was sterilized with 70% v/v ethanol and rinsed with sterile MilliQ water between each use. Positive growth was indicated by the pH indicator transitioning from a greyish blue (pH > 3) to yellow (pH < 3), indicating acid generation as a result of S oxidation.

3.3.4 Fe^{3+}-Reducing Bacteria

Heterotrophic, Fe (III)-reducing bacteria were grown in M1 Medium for Fe-reducing bacteria as outlined by Burlage et al. (1998). Sodium acetate was used as a carbon substrate such that the final concentration was 10 mM and Fe-citrate was used as an electron acceptor such that

the final concentration was 50 mM. In addition, the media consisted of 0.05% yeast to stimulate heterotrophic growth. Positive growth was indicated by Fe (II)-precipitates precipitating out of the media solution (initially brown media turns clear).

3.3.5 Acidophilic Fe^{2+}-Oxidizing Bacteria

Chemolithotrophic, Fe (II)-oxidizing bacteria were grown in ATCC 2039 *Acidithiobacillus ferroxidans* medium. The chemicals that comprise Part A of the media were added to 1 L of tap water and the pH was adjusted using a bench top pH meter to pH 2.3 using 0.1 N H_2SO_4 to prevent the Fe (II) from abiotically oxidizing once added. $FeSO_4 \bullet 7H_2O$ (electron donor) was quickly added and the solution was immediately filter-sterilized using a Nalgene vacuum filter tower (0.22µm) for sterility. Positive growth was determined by an increase in turbidity and a colour shift from a clear solution to orange/dark yellow with a distinct band indicating generation of Fe^{3+}.

3.4 X-Ray Diffraction Analysis

X-ray diffraction analysis (XRD) was conducted to gain an understanding of the mineralogy of the CT and whether it changed with depth in the CT deposit. Fe and S mineral phases were of interest and were therefore specifically targeted. Difficulties were encountered with XRD during analysis of the October 2011 field samples due to the high quartz content (> 60% of bulk mineralogy), thus, we strived to eliminate the quartz fraction when analyzing the December 2012 samples allowing for greater detection of less abundant minerals. CT samples

were suspended in degassed MilliQ water whereby the heavier quartz minerals quickly settled out of suspension and the overlying murky water was decanted for sample preparation. Samples were prepared by (1) eliminating the quartz fraction via suspension in degassed MilliQ water (described above); (2) air-drying the decanted waters in an anaerobic chamber in plastic weight boats to preserve oxygen sensitive mineral complexes; and (3) finely grinding samples using an acid-clean agate mortar and pestle. Samples were analysed at the McMaster University X-Ray Diffraction Facility (McMaster University, Hamilton, Ontario, Canada) using a high resolution Bruker D8 Advance Powder Diffractometer with a germanium monochormator. Samples were exposed to copper Kα1 radiation at 40lV and 40mA at a scan speed of 0.1 degrees 2θ per minute, with a step of 0.04 degrees and step time of 35 seconds. These data were analyzed with DFFRAC PLUS Evaluation software.

3.5 Organic & Inorganic Carbon Analysis

Analysis of the C content available in different phases of the study system can provide insight as to which microbial processes may be occurring, carbon limitations and carbon availability to microbes. Dissolved inorganic C (DIC) and dissolved organic C (DOC) were analyzed on the pore waters extracted from the CT field samples. Solid phase total organic C (TOC) and total inorganic C (TIC) were analyzed on each of the CT field samples.

All glassware (DOC vials, sample collection containers) were scrubbed with Extran® 300 detergent (Millipore, Darmstadt, Germany) and rinsed thoroughly with distilled H_2O. Glassware was soaked in a 10% HCl acid bath overnight (8+ hours), rinsed 7+ times with MilliQ water and allowed to dry. Any openings were sealed with aluminum foil and glassware was heated to 450°C in a muffle furnace for 8 hours. Upon use, DOC vials were sealed with

Teflon/silicone septa (Fisher Scientific) that were rinsed in a mixture of equal parts dimethylchloride/hexane/methanol and left to evaporate until dry. All ceramic combustion boats were scrubbed with Extran® 300 detergent, rinsed thoroughly with distilled water, then heated in a muffle furnace to 900°C for 20 minutes to burn off any residual carbon and stored in tin foil until use.

3.5.1 Porewater Analysis

Water was extracted from the CT porewater peepers (3 mL Slide-a-Lyzers filled with degassed MilliQ water) after 4 days of equilibration back in the laboratory in an anaerobic chamber, passed through a 0.7 µm filter and dispensed into C-free glass vials, sealed with a C-free septa and frozen at -20°C until analysis (< 28 days). All results were compared against a procedural blank of MilliQ water left to sit in a Slide-a-Lyzer peeper for 2 weeks and subjected to the same extraction procedure. Analyses were conducted in duplicate using a Shimadzu TOC-L Total Organic Carbon Analyzer with an autosampler ASI-L (Mandel Scientific, Guelph, Ontario, Canada) using the 680°C combustion catalytic oxidation method as per manufacturer recommended protocols. All samples were compared against a corresponding standard curve for either total C or inorganic C with a correlation value (R^2) of 0.99 or higher. Total C standards were prepared from a 1000 mg/L stock solution of potassium hydrogen phthalate (Sigma Aldrich) and all inorganic C standards were prepared from a 1000 mg C/L stock solution of 3.5 g $NaHCO_3$ and 4.41 g Na_2CO_3 (Sigma Aldrich) prepared in 1 L volumetric flasks. Standard curves were made fresh at the time of each analysis. Organic carbon values were obtained by subtracting the inorganic C values from the total C values.

3.5.2 Solid Analysis

The TOC and TIC content of the solid phase of the system was studied in addition to porewater samples. All sediments were collected in C-free glass jars and sealed with tin foil. Sediments were air-dried in an anaerobic chamber in aluminum dishes and finely ground using a C-free ceramic mortar and pestle (muffled at 900°C for 20 minutes). Sediments were analyzed for total C (TC) and TIC content using a Shimadzu TOC-L Total Organic Carbon Analyzer with a solid sampler SSM-5000A attachment (Mandel Scientific). Samples subject to TIC analysis were first equilibrated inside the sample chamber for 2 minutes to eliminate interference from atmospheric CO_2, then 0.5 mL of 50% H_3PO_4 acid was dispensed onto the sample using an automated dispenser and the sample was immediately loaded into the analysis chamber (200°C) where C was oxidized and the evolved CO_2 was measured using an infrared gas analyzer. Samples for TC analysis were directly loaded into the analysis chamber (900°C) where any C present was oxidized and the evolved CO_2 was measured using an infrared gas analyzer (Shimadzu Corporation, 2013). As per the machines detection limits, all samples subjected for analysis were less than 1 g and contained less than 30 mg of C. All analyses were conducted in C-free ceramic combustion boats and sample weights were determined using an analytical balance (Mettler-Toledo International Inc., Mississauga, Ontario, Canada). All samples were compared against standard curves made using known concentrations of glucose (TC analysis) or sodium carbonate (TIC analysis) and blank analyses (an empty C-free combustion boat). TOC values were obtained by subtracting TIC values from TC values.

3.6 Fe Sequential Extractions

In order to provide some insight into the occurrence and availability of Fe pools throughout the sediments microbial Fe metabolism, CT samples underwent a multi-step microwave digestion sequential extraction to target and analyze Fe pools present throughout the CT deposit. This procedure involved applying a sequence of progressively stronger reagents to a sediment sample in order to fractionate Fe into operationally defined phases (Haack and Warren, 2003). Typically this type of sequential extraction is used to sequentially dissolve sediment phases important in the sequestration of metals after the initial weak surface leach step, i.e. carbonates/acid soluble sulphides, amorphous Fe^{3+} oxyhydroxides, crystalline Fe^{3+} oxides, organics/sulphides and recalcitrant minerals. Here, in particular, the quantities of bioaccessible Fe^{3+} phases in the CT were of interest, i.e. the amorphous and crystalline Fe^{3+} phases, as these would potentially support iron reducing bacteria (IRB) potentially enabling the formation of FeS precipitates.

Sediments were air-dried in an anaerobic chamber in covered plastic dishes to preserve any oxygen-sensitive phases and ground using an acid-clean agate mortar and pestle (Donisa, et al., 2008). Sequential extractions were conducted in triplicate, where 0.5 - 1 g of dried sediment was added to each acid-clean 40 mL centrifuge tube. Twenty millilitres of reagent was added to each centrifuge tube and subjected to the extraction method outlined in Table 3.3 in the according sequence. Samples were microwaved using an Ethos Plus Microwave Labstation (Milestone Microwave Laboratory Systems, Sorisole, Italy) and centrifuged at 8000 RPM for 15 minutes in a Sorvall RC 5C Plus centrifuge (Mandel Scientific). The supernatant from each digestion step was decanted into separate trace metal free 50 mL Falcon tubes and preserved with 2% concentrated trace metal grade HNO_3.

Table 0.3. Outline of the reagents, sediment phase targeted and extraction method used for the microwave digestion sequential extraction technique (Haack and Warren, 2003).

Fraction	Reagent	Method
1: Easily Exchangeable	1 M sodium acetate, pH = 8.2 (with HOAc)	1 hr shaking, room temperature
2: Acid Soluble	1 M sodium acetate, pH = 5 (with HOAc)	Microwave Program 1 (MP-1): heat to 150°C over 8 min; maintain temperature for 5 min; 30 min cool-down
3: "Amorphous Oxyhydroxides"	0.25 M hydroxylamine hydrochloride in 0.25 M HCl	MP-1
4: "Crystalline Oxyhydroxides"	0.25 M hydroxylamine hydrochloric in 25% v/v acetic acid	MP-1
5: "Organics and Sulfides"	3:2 ratio 30% H_2O_2: 0.02 M HNO_3 + 1:4 ratio 3.2 M NH_3OAc:MilliQ water	MP-1
6: Residual	Concentrated HNO_3	Microwave Program 2 (MP-2): heat to 180°C over 20 min; maintain temperature for 10 min; 45 min cool-down

Concentrations of Fe in each fraction were determined spectrophotometrically using an Ultraspec 3000 UV /Visible spectrophotometer in conjunction with FerroVer total Fe quantification method (Hach Company) following the manufacturer supplied protocol, in triplicate. Absorbance values were translated to concentrations based on a standard curve generated using a known solution of iron chloride (Fisher Scientific). All equipment was soaked in a 4% HCl acid bath for 8+ hours and rinsed 7 times with MilliQ water prior to use and between uses.

3.7 Microbial Community Analysis

3.7.1 16S rRNA Sequencing

Bulk community DNA from each depth of CT sampled and the drill water was extracted aseptically in a BSC using the PowerSoils™ DNA Isolation Kit (Mo Bio Laboratories, Carlsbad, CA, USA) following the manufacturer-supplied protocol with low biomass modifications. DNA was stored in 10 mM Tris buffer at -80°C until it was submitted for 454 pyrosequencing to Mr. DNA Next Generation Sequencing and Bioinformatics Services (Shallowater, Texas, USA). The 16S bacterial gene was targeted using the universal Eubacterial primers 27F (5'-AGRGTTTGATCMTGGCTCAG – 3') and 530R (5'-CCGCNGCNGCTGGCAC – 3') and PCR was conducted using the HotStarTaq Plus Master Mix Kit (Qiagen, USA), through which samples underwent the following conditions: 94°C for 3 minutes, followed by 28 cycles of 94°C for 30 seconds, 53°C for 40 seconds and 72°C for 1 minutes with a final elongation step at 72°C for 5 minutes. Sequencing was performed using the Roche 454 FLX genome sequencer system and FLX Titanium reagents (Roche Applied Sciences, IN, USA). Data was processed using a proprietary analysis pipeline where data was depleted of barcodes and primers, sequences were denoised, operational taxonomic units (OTUs) were generated (binned at 97% similarity) and chimeras removed (MRDNA, Shallowater, TX, USA). Sequences were classified using the Basic Local Alignment Search Tool for nucleotides (BLASTn) and compared against a compiled GreenGenes database and analyzed for community composition (Dowd, et al., 2008; Wolcott, et al., 2009). Drill water sequences were deleted from the CT sequences at the genus level to account for drill water contamination during field sampling. All sequences were aligned using the RDP pipeline alignment tool and phylogenetic trees were generated using FastTree (Price, et al., 2009).

3.7.2 Analysis of Microbial Community Structure

The UniFrac web application (http://bmf.colorado.edu/unifrac (Lozupone & Knight, 2005; Lozupone, et al., 2006)) was used to evaluate microbial community structure with depth within the CT deposit. UniFrac is a phylogenetic distance metric which accounts for the different degrees of similarity between 16S rRNA gene sequences in a phylogenetic tree and thus gathers more information than comparable taxon-based metrics that bin 16S rRNA genes based on 97-99% similarity (Bouzat, et al., 2013; Elliot & Warren, 2013). Cluster environment analysis, community significance tests and principal component analysis (PCA) analysis were conducted using UniFrac (Lozupone, et al., 2006). Principal components were subsequently compared against environmental parameters to determine any driving factors behind microbial community spatial structuring.

3.8 Statistical Analysis

Statistical analyses were used to assess if significant differences occurred down core in the CT deposit with both geochemical and microbiological datasets. Whenever possible analyses were conducted in triplicate and standard deviations were calculated. Error bars on all graphs represent one standard deviation. Significance of porewater and solid phase trends with depth were tested using one way ANOVA tests while two-tailed correlations were used to compare UniFrac PCA and environmental variables. All statistical analyses were conducted using the IBM SPSS Statistics 21 software package and tests were considered significant at $\alpha = 0.05$, unless otherwise noted.

RESULTS AND DISCUSSION

This chapter is in preparation for submission as an original manuscript to

Environmental Science & Technology for review.

Microbial Sulfur Biogeochemistry of Athabasca Region Oil Sands Composite Tailings

Kathryn E. Kendra and Lesley A. Warren

Abstract

While the biogeochemistry of base metal mining wastes, i.e. acid mine drainage (AMD) contexts have been well studied, this is the first study assessing the biogeochemistry of composite tailings (CT), a sulfur- and organic-rich, circumneutral, brackish waste material resulting from surface mining activities in Alberta's oil sands. Deep subsurface samples were collected for geochemical and molecular microbiological analyses at 2 meter intervals over 36 meters of depth within a CT deposit slated for reclamation. Results identify that percentages of Fe-bearing minerals and organic C increase with depth while acid-soluble sulfide and sulfate were invariant. Porewater [H_2S] was widespread throughout the deeper depths of the deposit (up to 301.5 µM, > 6 m) with surface limited occurrence of Fe^{2+} (up to 38.5 µM, < 6 m). Currently, [Fe^{2+}] generated within the CT deposit is sufficient to sequester the ambient H_2S generated, thus mitigating the potential for outgassing. Metagenomic characterization revealed highly diverse CT microbial communities (over 20 different phyla) with highest diversities associated with the depth of highest [H_2S] and depth of joint Fe^{2+}/H_2S occurrence. Positive growth for SRB enrichments as well as the occurrence of 10 known SRB genera identify the importance of microbial S reduction in these materials. Multivariate PCA analyses (Unifrac) identified DOC, ORP and salinity to be the major drivers of bacterial community composition and structuring corresponded with zones of Fe^{3+} reduction or SO_4^{2-} reduction.

Keywords: oil sands, composite tailings, sulfur biogeochemistry, metagenomics

Introduction

Composite tailings (CT) are a semi-solid, brackish, circumneutral waste material that results from surface mining activities in Alberta's oil sands. CT is comprised of a mixture of 18% oil sands tailings and 82% post-processed sand, amended with gypsum ($CaSO_4 \bullet 2H_2O$), a flocculating agent, which results in a dense, sulfur and organic rich waste residue material capable of supporting reclamation landscapes. Alberta government legislation requires that any land disturbed by mining activity be reclaimed and restored to its natural state, as such, CT is currently used to in-fill abandoned mine pits resulting in extensive deposits over 36 m deep (Syncrude Canada Ltd, 2010; Government of Alberta, 2013). With Alberta's oil sands spanning a 4,800 km^2 area and current production exceeding 800,000 barrels of bitumen per day, tailings-based landscapes will become increasingly prevalent with the potential for as yet unknown environmental impacts (Voordouw, 2012; Government of Alberta, 2013).

Sulfur (S) cycling, widespread across wetland, groundwater, oceanic, lacustrine and mining environments plays an integral role in globally important biogeochemical processes such as carbon mineralization, water/soil acidification, pyrite formation and hydrogen sulfide (H_2S) gas release (D'Hondt, et al., 2004; Bernier & Warren, 2005; Morse, et al., 2007). S cycling is dynamic and variable across environments due to differences in key factors affecting S transformations such as pH, temperature, redox status, salinity, organic carbon (OC) content, the nature and concentrations of S containing solids as well as the types and rates of microbial metabolism (e.g. S reduction, S oxidation and S disproportionation). Additionally, S cycling is tightly coupled with and controlled by iron (Fe) dynamics though mineral precipitation and weathering (i.e. pyrite and pyrrhotite) (Thamdrup, et al., 1994; Zhu, et al., 2012).

S cycling has been extensively investigated across natural systems (e.g. lakes, bogs, marine, etc.) and has illustrated the important role that microbial S transformations play. To date, most S-based mining investigation has focused on microbially driven generation of acid mine drainage (AMD) associated with base metal mining activities, i.e. typically organic poor, acidic and metal rich contexts (Edwards, et al., 2000). However, recent research has provided evidence of increasing S emissions from the oil sands with well-established communities of sulfate reducing bacteria (SRB) and measurable H_2S concentrations occurring in oil sands tailings (Gieg, et al., 2010; Penner & Foght, 2010; Harner, et al., 2011; Ramos-Padron, et al., 2011; Proemse, et al., 2012; Fru, et al., 2013). To date, microbially-mediated methanogenesis in tailings lakes has been the focus of oil sands microbial geochemical investigations (Penner & Foght, 2010; Siddique, et al., 2012; Saidi-Mehrabad, et al., 2013). Microbial characterization of the tailings materials has revealed unexpectedly high microbial diversity; with established communities of SRB (10^4 cells/mL) occurring in addition to the expected methanogens (Penner & Foght, 2010), supporting the notion that active S cycling occurs in these materials. Indeed, the addition of gypsum to tailings ponds has stimulated SRB, resulting in the inhibition of methanogenesis (Harner, et al., 2011; Ramos-Padron, et al., 2011; Fru, et al., 2013). Thus, CT, composed of tailings, gypsum and post- processed sand, is likely to host microbially diverse communities where the circumneutral pH and additions of solid SO_4^{2-} (gypsum) favour SRB metabolism with the potential for H_2S generation. No research to date has investigated the microbial community structure and solid/porewater S geochemistry within oil sands CT deposits. Thus, the objectives of this study are to (1) characterize the solid and porewater S/Fe geochemistry of CT with depth,

and (2) investigate the associated microbial communities with depth and assess the role they may have in biogeochemical S cycling within CT.

Methods

Site Description and Sampling Strategy

Samples were collected from the Kingfisher CT deposit located in the northwest corner of the East-in-Pit tailings deposit at Syncrude Canada Ltd. in December 2012. The Kingfisher CT deposit spans a 1.12 km^2 area and consists of a retired open-pit mine site, ~ 40 m deep, which has been in-filled with interbedded CT and tailings sand layers. CT liquefies upon disturbance due to the high water content, thus, unique sampling strategies were employed. Sampling of deep CT was facilitated through the use of an amphibious Fraste ML drill rig fitted with a sonic drill head using an AquaLock Piston Sampler which enabled sample collection and retention during extraction. CT was collected in ~ 2 m intervals over 36 m of depth where each interval was homogenized prior to sample distribution, thus, all analyses here represent a bulk characterization over a 2 m depth interval. Drill cores were directly extruded into a sterile N_2-filled anaerobic glove bag, homogenized and aliquoted for analyses. Geochemical screening was conducted over 2 m increments through the deposit where pH, temperature, ORP and conductivity were measured and samples were screened for H_2S through colorimetric assessment using methylene blue (Method 8131, Hach Company) and lead acetate paper (Sigma Aldrich). Based on the initial screening, five depths were selected for in-depth analyses (2-4 m, 6-8 m, 14-16 m, 22-24 m and 32-34 m) where samples were collected for: (1) solid-phase Fe and S analysis, TOC/TIC and bulk mineralogy; (2) analysis of porewater Fe and S species and DOC/DIC; and (3) metagenomic microbial community analysis and (4) functional enrichment

assessment for SRB, S oxidizing bacteria (SOB), iron reducing bacteria (IRB) and iron oxidizing bacteria (IOB).

Solid Phase Sample Collection and Analysis

Upon sample collection, CT was aliquoted into Whirlpak bags or C-free glass jars (soaked in 10% HCl for > 8 h and rinsed with ultrapure water (18.2 Ω. m cm^{-1}, Milli-Q, Millipore) and heated to 450°C for 8 h) and preserved anaerobically in Mylar bags with oxygen absorbing packets (Canadian Survival Company) at -20°C until analysis. All CT samples were air-dried in an anaerobic chamber and finely ground prior to analysis. Given the highly altered nature of the CT materials, in addition to classic mineralogical analyses (XRD), a modified Tessier sequential extraction method was used operationally assess [Fe] associated with different components of the solid phase CT materials (Haack & Warren, 2003). Triplicate CT solid samples were analyzed, partitioning [Fe] into six operationally defined fractions: easily exchangeable (loosely bound), acid soluble, easily reducible (amorphous Fe^{3+} oxyhydroxides), reducible (crystalline Fe^{3+} oxides), oxidizible (organics and/or sulfides) and residual (resistate minerals). Concentrations of Fe in each phase were determined colorometrically in triplicate using the Ferrover HACH method (Ultraspec 2000, UV/visible spectrophotometer, Pharmacia Biotech, Cambridge, UK). Background contamination was accounted for through procedural blanks and was found to be negligible (< 5%). Total sediment Fe concentrations were calculated through the sum of Fe concentrations across the six fractions while the proportion of bioavailable $Fe^{(III)}$ (e.g. available to iron reducing bacteria, IRB) was approximated through the sum of Fe concentrations in the easily reducible and reducible fractions (fractions outlined by (Haack & Warren, 2003). Solid-phase S species were quantified through acid volatile sulfide analysis (AVS, i.e. reduced S

phases) and acid extractable sulfate (AES) analysis using a method adapted from Burton et al. (2007) and Hsieh et al. (2002). Sulfide and sulfate concentrations were determined colorometrically using the Sulfide and SulfaVer HACH methods respectively (Ultraspec 2000), and were normalized to sediment weight. Sediment C contents (TOC/TIC) were analyzed on a Shimadzu TOC-L Analyzer with a Solid Sample Combustion Unit (Mandel Scientific) using the 680°C combustion catalytic oxidation method (ShimadzuCorporation, 2013). X-ray diffractometry (XRD) was used to determine the bulk mineralogy of the CT with depth. Samples were analyzed by the McMaster University X-Ray Diffraction Facility with emphasis on Fe and S mineral phases (Brockhouse Institute for Materials Research, McMaster University, Hamilton, Ontario).

Analysis of CT Porewaters

As CT is an unstable material with a high fines content that liquefies easily, preventing the collection of dissolved porewater samples through filtration or settling in the field, Slide-a-Lyzer cassettes (Thermo Scientific, 3 mL volume with a 20 kDa MWCO) equipped with dialysis membranes were used to separate porewaters. CT was extruded within an Atmosbag glove bag under N_2 gas and aliquoted into Whirlpak bags containing Slide-a-Lyzers pre-filled with degassed ultrapure water and preserved anaerobically at 4°C until analysis. Slide-a-Lyzers were equilibrated with CT for 4 days (experimentally determined) at which point the water was anaerobically extracted from the Slide-a-Lyzers and analyzed for [$\sum H_2S$], [SO_4^{2-}], [$Fe^{(II)}$] and [$Fe^{(III)}$] (quantified using reagents and manufacturer supplied protocols from Hach Company with Ultraspec 2000). Samples extracted from Slide-a-Lyzers for porewater DOC/DIC analysis were filtered (0.7 µm) into C-clean glass vials and frozen at -20°C until analysis (< 28 days).

Carbon concentrations (DOC/DIC) were measured on a Shimadzu TOC-L analyzer (Mandel Scientific) and procedural blanks accounting for background C contamination were insignificant (DOC < 25%, DIC < 1%). Geochemical equilibrium modelling using PHREEQC Version 2.18 (USGS, http://wwwbrr.cr.usgs.gov/projects/GWC_coupled/phreeqc/ index.html) was used to determine the speciation of H_2S within porewaters.

DNA Extraction and Analysis of Pyrosequencing Data

Total community DNA was extracted from CT sediment samples and drill water (to assess any contamination) using the PowerSoils™ DNA Isolation Kit (Mo Bio Laboratories, Carlsbad, CA, USA) using low biomass modifications. Samples were submitted for pyrosequencing to Mr. DNA Next Generation Sequencing and Bioinformatics Services (Shallowater, TX, USA). Polymerase chain reaction (PCR) was performed using the universal Eubacterial primers 27F (5'AGRGTTTGATCMTGGCTCAG-3') and 530R (5'-CCGCNGCNGCTGGCAC-3') in which samples were subjected to the following conditions: 28 cycles of 94°C (30 s), 53°C (40 s) and 72°C (60 s) with a final elongation step at 72°C (300 s). Sequencing was performed using the Roche 454 FLX genome sequencer system with FLX Titanium reagents (Roche Applied Sciences, IN, USA) as previous described (Dowd, et al., 2008; Wolcott, et al., 2009). Data was processed using a proprietary analysis pipeline where data was depleted of barcodes and primers, sequences were denoised, chimeras were removed and operational taxonomic units (OTUs) were generated (binned at 97% similarity). Sequences were classified using BLASTn, compared against a complied GreenGenes database and analyzed for community composition. Drill water sequences were removed from CT sequences at the genus level to account for drill water contamination during field sampling. Sequences were aligned using the Ribosomal Database

Project Pyrosequencing Alignment tool and a phylogenetic tree was generated using FastTree (Cole, et al., 2009; Price, et al., 2009). Bacterial community cluster analysis and principal components analysis (PCA) was conducted using UniFrac (http://bmf.colorado.edu/unifrac (Lozupone, et al., 2006)). All correlations were calculated at a significance level of α=0.05 (two-tailed) unless otherwise specified using SPSS statistical software.

Microbial Enrichments

In addition to genetic characterization, functional enrichments for Fe and S-metabolising bacteria were employed to establish the potential for these metabolisms to occur within the communities sampled following well-established protocols. Two depths, 6-8 m and 22-24 m, were selected for enrichments. CT from 6-8 m was enriched for SRB, IRB, SOB and IOB. SRB were grown on a lactate media as outlined by Burlage et al. (1998). Positive SRB growth was indicated by the formation of a black FeS precipitate. Fe (III)-reducing bacteria were grown in M1 Medium for IRB as outlined by Burlage et al. (1998). Sodium acetate was used as a carbon substrate such that the final concentration was 10 mM and Fe-citrate was used as an electron acceptor such that the final concentration was 50 mM. Positive growth was indicated by Fe (II)-precipitates precipitating out of the media solution (initially brown media turns clear). Acidophilic SOB were grown on a modified ATCC 125 media using tetrathionate ($S_4O_6^{2-}$) as an electron donor. Acid generation (pH < 3) indicated positive growth. Neutrophilic SOB were grown on a thiosulfate ($S_2O_3^{2-}$) media as outlined by Burlage et al. (1998) where acid generation (pH < 8) indicated positive growth. IOB were grown on ATCC 2039 medium for *Acidithiobacillus ferroxidans* where positive growth was indicated by an increase in turbidity and the development

of a distinct orange band (Fe^{3+}). All enrichments were carried out in an anaerobic chamber with all surfaces sterilized with 70% v/v ethanol prior to use.

Statistical Analyses

Statistical analyses were used to assess if significant differences occurred down core in the CT deposit with both geochemical and microbiological datasets. All analyses were conducted in triplicate and standard deviations (SD) were calculated. Error bars on all graphs represent one standard deviation. Significance of porewater and solid phase trends with depth were tested using one way ANOVA tests while two-tailed correlations were used to compare UniFrac PCA and environmental variables (IBM SPSS Statistic 21 software package).

Results and Discussion

CT Geochemistry

Depth dependent geochemical profiles through the 36 m of CT revealed saline, circumneutral pH, highly reducing, and warm materials even during winter sampling (Figure 4.1). pH showed a pronounced shallow decrease from 8.29 near the surface (2-4 m) to 7.21 at 4-6 m followed by a subsequent increase to 8.22 at 10-12 m with a steady decline to 7.37 at 26-28 m and a slight increase again to 7.81 at the bottom of the deposit (34 – 36 m) (Figure 4.1). CT pH values are thus comparable to marine sediments, seawater and oil sands tailings (Penner & Foght, 2010; Voordouw, 2012; Roychoudhury, et al., 2013). Temperature increased with depth (3.5 – 14.3°C), which has also been observed in tailings ponds and likely reflects the effects of increased pressure and thermal protection from surface cooling with depth (Penner & Foght,

2010). ORP values decreased from -90 mV near the surface (2-4 m) to -538 mV at depth (34-36 m) but displayed variability down core atypical of more consolidated, natural sediments and soils. Conductivity also varied with depth ranging from 1373 µS/cm (4-6 m) to 354 µS/cm (24-26 m), indicating salinities of ~ 1/2 to 1/15 times that of seawater (Mille, et al., 1991; Roychoudhury, et al., 2013). Variability in the geochemical profiles likely reflects the unstable and highly anthropogenically impacted nature of CT materials and infilling practices.

Porewater Fe^{2+}, suggestive of IRB activity, was detected in the two shallower depths sampled, 2-4 m and 6-8 m, at concentrations of 38.5 µM and 1.2 µM respectively (Figure 4.2, Table 4.1) and was comparable to reported [Fe^{2+}] for Arctic marine sediments (20 – 47 µM; Algora, et al., 2012) but considerably higher than those reported for oil sands tailings (0.36 to 10.9 µM; Penner & Foght, 2010). Porewater $\sum H_2S$ was detected at the four deeper depths sampled (6-8 m, 14-16 m, 22-24 m and 32-24 m). The highest porewater [H_2S] of 301.5 µM occurred at 22-24 m, which was significantly higher than any other depth sampled ($p < 0.01$), which ranged from 14 – 23 µM (Figure 4.2, Table 4.1). These H_2S values are greater than those reported for tidally reflooded wetlands and peatlands (< 2 µM to 9 µM; Blodau, et al., 2007; Burton, et al., 2011a) and the 22-24 m depth demonstrates [H_2S] similar to those reported from oil sand tailings bioreactor experiments (< 150 µM; Fru, et al., 2013), SO_4^{2-} amended microcosm experiments (400 µM; Salloum, et al., 2002) and brackish coastal lake sediments (ranged from 3 – 1380 µM; Sakai, et al., 2013).

Dissolved porewater SO_4^{2-} was variable with depth ranging from 0 µM (32-34 m depth) to 0.79 µM (2-4 m depth) indicating that porewater SO_4^{2-} is available in low concentrations throughout

the CT above 32-34 m of depth (Figure 4.2, Table 4.1). Measured SO_4^{2-} in CT is considerably less than that measured *in situ* in oil sands tailings lakes (Penner & Foght, 2010) and marine sediments (Algora, et al., 2013), suggesting the gypsum amendment is highly insoluble. Considering that ~1400 g of gypsum are added per cubic meter of tailings to form CT (Matthews, et al., 2002) and that the SO_4^{2-} molecule accounts for 56% w/w of gypsum, < 4% of SO_4^{2-} that has been added to the system has been converted to H_2S based on a 1:1 mole ratio (Equation 12). High concentrations of porewater DOC were measured throughout the depth

$$SO_4^{2-} + CH_2O \leftrightarrow H_2S + CO_2 \quad (12)$$

profile, nearly three times higher than those reported previously for oil sands tailings (Penner & Foght, 2010), ranging from 84.9 - 146.4 mg/L with an exception at 22-24 m where the concentration dropped to 27.1 mg/L, which interestingly corresponds with the highest porewater [H_2S] (301.5 µM) (Figure 4.2, Table 4.1).

XRD investigation of the solid phase mineralogy revealed variable composition with depth where only 35-65% of the total mineralogy was accounted for with the highest yields at the two deepest depths sampled (63-65% yield); this low yield could reflect the heterogeneous, highly anthropogenically altered nature of CT materials, the removal of the quartz fraction prior to analysis or the organic content of these materials. Mineralogical analyses revealed Fe-bearing minerals (i.e. siderite (Fe^{2+}; $FeCO_3$), goerthite (Fe^{3+}; α-FeO(OH)), magnetite (Fe^{2+}/Fe^{3+}; Fe_3O_4) and Fe-rich clays) account for ~20 - 50% of the overall CT mineralogy with proportions of Fe^{2+}-bearing minerals increasing down core (siderite increased from 8% to 13%; magnetite increased

from 8% to 14%) (Table 4.2). These mineralogical results were supported by Fe sequential extraction results which indicated solid phase Fe (total; ∑ of all extraction fractions) and bioavailable ferric Fe (i.e. Fe^{3+} phases) concentrations increased with depth (R^2 = 0.93 and 0.96 respectively, $p < 0.05$) where total Fe doubled from 35.9 to 73.4 µmol/g as did the bioavailable portion from 22.6 to 47.2 µmol/g (Table 4.3). Approximately 64% of total extractable Fe was bioavailable based on the sequential extraction results for the easily reducible (amorphous oxyhydroxides) and reducible (crystalline (hydr)oxides) fractions (i.e. Fe^{3+} phases). However,

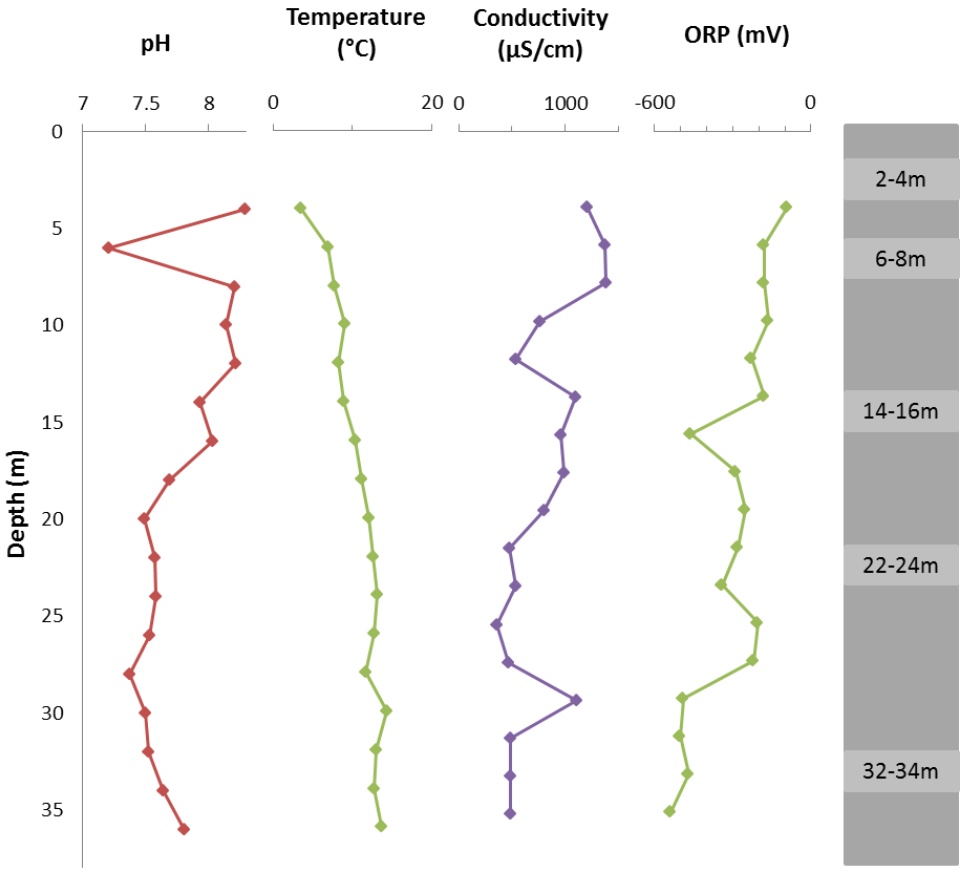

Figure 4.1. Geochemical profiles for pH, °C, conductivity and ORP over 36 m within the CT deposit.

the presence of porewater [Fe^{2+}] detected only within the shallower depths of the CT deposit sampled (< 8 m) despite the presence of Fe^{3+} minerals down core suggests that these Fe-bearing phases may not be easily accessible to the IRB microbial community and/or other characteristics or factors present at depth inhibit IRB activity (e.g. C sources, out competition by SRB). CT [OC] exhibited a significant increase with depth ($R^2 = 0.8$, $p < 0.05$) increasing from 0.79 to 1.22% of total solids, by weight (Table 4.3). These values are consistent with the residual bitumen and naphtha content of the original tailings materials incorporated into CT, which range from 1.1 – 2.6% and 0.02 – 0.25%, respectively (Penner & Foght, 2010). Similar OC values have been reported in coastal marine sediments ranging from 0.5 – 1.2% w/w and in both artificial and natural wetlands ranging from 1.1 – 2.5% w/w (Zhu, et al., 2012; Peralta, et al., 2013). Interestingly, no S minerals were detected by XRD, despite the gypsum addition to CT (~1400 g/m^3), and AVS and AES concentrations were low, with AVS concentrations ranging from 0.43 – 0.51 µmol/g and concentrations of AES ranging from 0.010 – 0.014 µmol/g with no significant differences down core (Table 4.3). Based on the solubility of gypsum ($K_{sp} = 10^{-4.5}$), we would expect for the majority of gypsum to be insoluble, thus suggesting that the representation of S minerals was below the detection limits of the methods used. Thus, additional factors not identified by our analyses appear to be controlling the behaviour and solubility of S minerals (i.e. gypsum) within this deposit.

The presence of both Fe^{2+} and H_2S at 6-8 m could be suggestive of co-occurring IRB and SRB metabolism within this region. Further at this depth, porewater [Fe^{2+}] and [H_2S] indicate supersaturation with respect to pyrite and undersaturation with respect to amorphous FeS

precipitates, pyrrhotite, mackinawite or greigite (Davison, 1991). The higher concentrations of $\sum H_2S$ observed at the deeper depths are also associated with decreasing pH indicating relatively greater abundance of the H_2S species. Equilibrium modeling using PHREEQC (USGS) of H_2S speciation indicated concentrations of H_2S ranging from 1.2 to 76.3 μM (22-24 m, Table 4.4, also lowest pH 7.58, Table 4.1). As this CT deposit is highly dynamic and anthropogenically altered, it is important to note that the porewater concentrations of Fe and S species measured at each depth are likely to be controlled by a combination of microbial processes (e.g. IRB/SRB metabolism) in conjunction with abiotic processes such as diffusion, forced dewatering of the materials and percolation of surficial inputs (e.g. runoff from an adjacent reclamation fen project).

Microbial Community Composition as a Function of Depth

The geochemical survey information and analyses (i.e. pH, ORP, mineralogy, total Fe, AVS, Figures 4.1 and 4.2, Tables 4.1 and 4.2) would not point to the high $[H_2S]$ observed at 22-24 m, supporting a microbial role in its generation. Further, the occurrence of both Fe^{2+} and H_2S at the 6-8 m depth, the inverse relationship between porewater $[H_2S]$ and [DOC] at 22-24 m in conjunction with the presence of the mixed valence Fe mineral magnetite over much of the deposit, which is frequently associated with microbial IRB activity (Fortin & Langley, 2005), strongly suggests that both Fe and S microbial cycling are occurring. Further, the results here suggest three zones of microbial activity with depth in the deposit: IRB (shallow), IRB and SRB (mid, 6-8m) and SRB (deeper) and thus the occurrence of functionally distinct microbial populations with depth.

A phylum-level survey of the bacterial community composition identified CT is dominated by Proteobacteria (specifically Betaproteobacteria and Gammaproteobacteria) accounting for 90-98% of the total community (Figure 4.3). Firmicutes (up to 6%), Chloroflexi (up to 6%), Spirochaetes (up to 3%) and Actinobacteria (up to 2%) were common across depths but present to lesser extents. Proteobacteria have also been found to dominate the bacterial community in oil sands tailings, AMD systems, marine sediments, freshwater lake sediment and wetlands, ranging from 40% to over 90% of the total community representation (Kim, et al., 2004; Penner & Foght, 2010; Siddique, et al., 2012; Auld, et al., 2013; Bouzat, et al., 2013; Peralta, et al., 2013; Reis, et al., 2013). Here, CT demonstrated high diversity with 20 different phyla encountered overall community percentage of 89.2%); this again correlates with the highest zone of H_2S observed with depth (Figure 4). The percentage of the total bacterial community within this CT deposit potentially capable of carrying out SO_4^{2-}-reduction was very high (greater than 90%), however Arctic marine sediments have also reported SRB accounting for up to 70% of total microorganisms detected (Algora, et al., 2013). Therefore, these results indicate that community representation of SRB could play a role in H_2S generation with depth.

Environmental microbial enrichments revealed positive growth for SRB, SOB and IRB at 6-8 m and positive growth of SRB and SOB at 22-24 m, which further confirms that these metabolisms are likely occurring within the deposit. Negative growth was observed for IOB at 6-8 m, which is consistent with the geochemical characterization in that limited pools of Fe^{2+} are available in CT to drive this metabolism and conditions are anoxic (nitrate concentrations unknown). Interestingly, positive growth of SOB was observed with depth. SOB are capable of utilizing Fe^{3+} as an electron donor, therefore, given that solid phase Fe^{3+} is readily available throughout

the CT deposit, this suggests that coupled S redox cycling is possible throughout depth. Additionally, due to the Fe^{3+} concentrations measured with depth, there is the potential for active Fe^{3+} reduction throughout CT if appropriately stimulated, which could impact S cycling through Fe-sulfide mineral precipitates. Despite the demonstrated functional capabilities for both Fe- and S-metabolism, the relative differences in the [H_2S] and [Fe^{2+}] between the two depths suggests *in situ* factors are differentially affecting IRB and SRB organisms ability to actively metabolize. Multivariate statistical analyses were used to compare the community composition across the five depths sampled. The Unifrac web application (http://bmf.colorado.edu/unifrac (Lozupone and Knight, 2005; Lozupone et al., 2006; Lozupone et al., 2007)) was used to evaluate microbial community structure with depth within the CT deposit. Unifrac is a phylogenetic distance metric which accounts for the different degrees of similarity between 16S rRNA gene sequences in a phylogenetic tree and thus gathers more information than comparable taxon-based metrics that bin 16S rRNA genes based on 97-99% similarity (Bouzat, et al., 2013; Elliot & Warren, 2013). UniFrac significance tests indicated distinctly unique microbial communities down core ($p < 0.01$) while cluster analysis revealed that depths with detectable H_2S were most similar and clustered together (Figure 4.5). Principal components PC1, PC2 and PC3 accounted for over 80% of the data variation and when plotted against each other, PC1 and PC2 revealed that 2-4 m is significantly different than the other four depths; 6-8 m, 14-16 m, 22-24 m and 32-34 m (Figure 4.5). This corresponded with zones where Fe^{3+} reduction was occurring (2-4 m) and zones where SO_4^{2-} reduction was occurring (14-16 m, 22-24 m and 32-32 m), identifying that the

Table 0.1. Complete porewater results for the five depths of CT sampled. Means were generated from triplicate analyses and one standard deviation (SD) of variance is shown. Parameters which yielded results below the detection limits are denotes with 'ND' for not detected.

Depth (m)	pH	Temp (°C)	ORP (mV)	EC (µS/cm)	$\sum H_2S$ (µM)		Fe^{2+} (µM)		Fe^{3+} (µM)	SO_4^{2-} (µM)		OC (mg/L)		IC (mg/L)	
					Mean	*±1 SD*	*Mean*	*±1 SD*	*Mean*	*Mean*	*±1 SD*	*Mean*	*±1 SD*	*Mean*	*±1 SD*
2-4	8.29	3.5	-89.5	1207	*ND*		38.5	33.5	*ND*	0.8	0.1	85.0	0.4	98.5	0.2
6-8	8.21	7.7	-178.9	1381	22.8	3.0	1.2	2.0	*ND*	0.3	0.1	84.9	1.1	159.0	0.5
14-16	8.03	10.4	-459.9	959	14.3	9.3	*ND*	*ND*	*ND*	0.1	0.0	85.6	0.4	185.7	0.5
22-24	7.58	13.1	-341.5	531	301.5	86.5	*ND*	*ND*	*ND*	0.2	0.2	27.1	0.4	255.8	1.0
32-34	7.64	12.7	-470.0	488	23.0	5.5	*ND*	*ND*	*ND*	0.0	0.0	146.4	*ND*	217.0	0.4

Table 0.2. XRD determined mineralogy of CT with depth.

Mineral	Depth of CT				
	2-4m	6-8m	14-16m	22-24m	32-34m
Quartz	2%	1%	2%	2%	2%
Calcite	1%	3%	3%	4%	3%
Albite/anorthite	4%	5%	6%	~5%	4%
Microcline	4%	2%	4%	3%	3%
Dolomite (ankerite)	1%	2%	1%	1%	2%
Goerthite	2%	3%	3%	2%	3%
Magnetite	8%	9%	~9%	14%	14%
Illite/micas	2%	3%	3%	4%	4%
Chlorite	1%	1%	1%	2%	2%
Halite	2%	2%	2%	2%	2%
Siderite	8%	~9%	10%	13%	12%
Kaolinite/serpentine	8%	~9%	10%	13%	12%
Amorphous, ect.	4%	4%	4%	5%	~5%

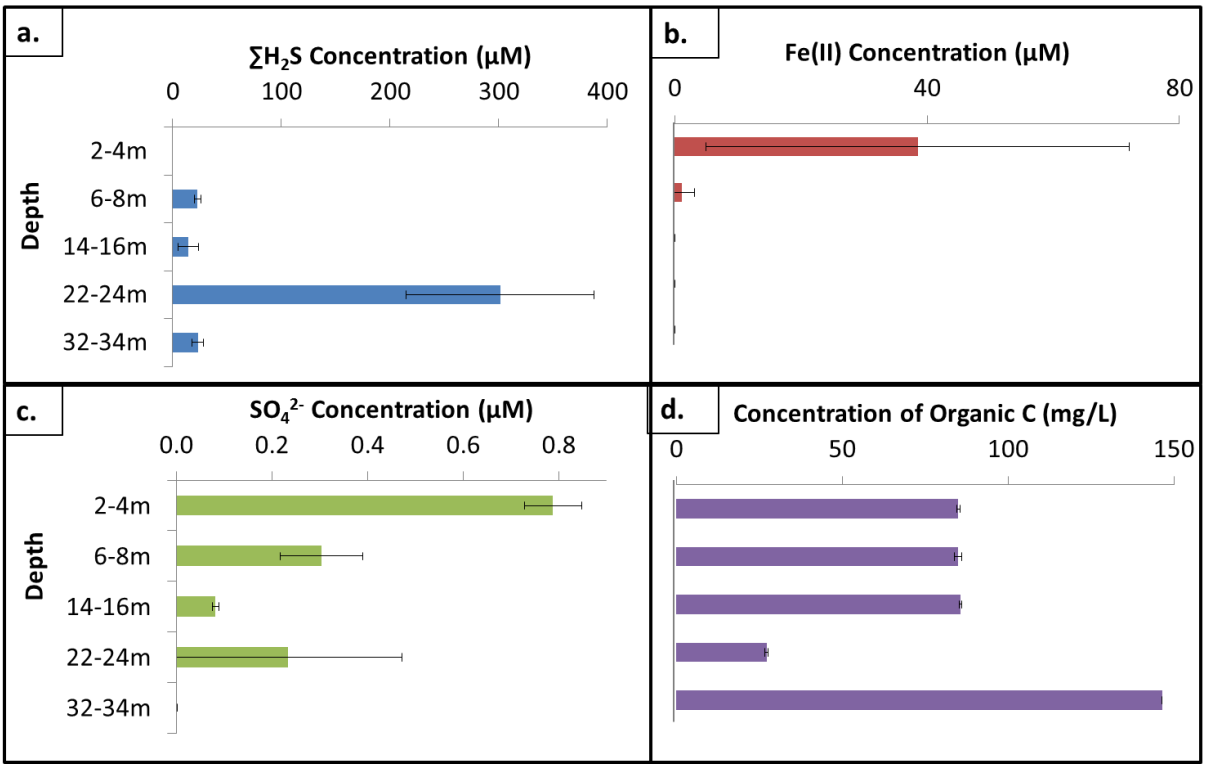

Figure 0.2. Porewater concentrations of (a) $\sum H_2S$, (b) Fe^{2+}, (c) SO_4^{2-} and (d) DOC with depth throughout the CT deposit. Values displayed are means generated from triplicate analyses with error bars representing one standard deviation of variance.

Table 0.3. Complete solid phase results of the five CT depths sampled. Means were generated based on triplicate analyses with one standard deviation (SD) of variance.

Depth (m)	% Organic C		Total Fe (µmol/g)		AVS (µmol/g)		AES (µmol/g)	
	Mean	*±1 SD*	*Mean*	*±1 SD*	*Mean*	*±1 SD*	*Mean*	*±1 SD*
2-4	0.79	0.28	35.41	1.03	0.428	0.007	0.014	0.007
6-8	0.75	0.15	39.38	9.24	0.532	0.008	0.010	0.002
14-16	0.87	0.20	40.56	3.33	0.508	0.019	0.010	0.001
22-24	0.94	0.07	61.88	3.43	0.488	0.063	0.012	0.000
32-34	1.22	0.02	72.66	5.59	0.427	0.018	0.012	0.005

Table 0.4. PHREEQC geochemical equilibrium modelling (USGS) of porewater $\sum H_2S$ speciation associated with the 5 sampling depths of the CT deposit.

Depth (m)	$\sum H_2S$ (µM)	Predicted Speciation		
		HS^- (µM)	H_2S (µM)	S^{2-} (µM)
2-4	0.00	0.00	0.00	0.00
6-8	22.78	20.52	1.94	0.00
14-16	14.29	12.60	1.17	0.00
22-24	301.50	225.31	76.28	0.00
32-34	23.03	17.69	5.34	0.00

SRB communities at these depths are important structural components. Interestingly, 6-8 m, where both Fe^{3+} reduction and SO_4^{2-} reduction were observed, clustered strongly with the other H_2S depths along PC1 but also shows some similarity to the Fe zone along PC2. PC1 demonstrated a weakly significant negative correlation ($p < 0.1$) with ORP and conductivity while PC2 revealed a significant negative correlation ($p < 0.05$) with DOC concentrations (Figure 4.5).

Given the interrelated nature of S and Fe cycling the community of bacteria capable of carrying out Fe reduction (IRB) was also investigated. The highest counts of putative IRB were found at 6-8 m and 22-24 m, where the analyses had indicated the greatest number of overall cells (Figure 4.6). Interestingly, the highest representative community percentage of IRB (in comparison to total number of cells at that depth) was observed at 2-4 m where 72.7% of the community was capable of Fe^{3+} reduction; this depth also evidenced the highest levels of porewater Fe^{2+} measured (38.5 µM) (Table 4.1). However, porewater Fe^{2+} was only detected in the upper two depths characterized, suggesting that microbial Fe reduction was confined within the upper

portion of the CT (2-4 m and 6-8 m) deposit despite ~65% of the total bacterial community putatively having the capacity for Fe^{3+} reduction over the entire deposit depth and the occurrence of Fe^{3+}-bearing minerals increasing with depth.

Thus, community structuring with depth appears to be predominantly driven by changes in ORP, conductivity and DOC concentrations and not substrate availability or pH. While redox conditions and DOC availability have been shown to shape microbial community structure and composition, salinity (derived from conductivity) has been shown to be the major factor affecting microbial community composition overruling extreme pH and temperatures across a wide range of environments including seawater, natural soils, hot springs, microbial mats and acidic springs (Eiler, et al., 2003; Lozupone & Knight, 2005; DeAngelis, et al., 2010).

Implications of CT Biogeochemistry

Despite the high OC content of oil sands tailings, much of that C is not considered to be labile and accessible to microbes (Penner & Foght, 2010). Based on the results of this study, it would seem that with depth, the CT SRB community may have a greater ability than the IRB community to utilize recalcitrant OC (e.g. bitumen, naphthenic acids) given the widespread occurrence of porewater [H_2S] and limited [Fe^{2+}] despite accessible pools of Fe^{3+} with depth. While both SRB and IRB have demonstrated an ability to metabolize more recalcitrant forms of OC such as hydrocarbon crude oil constituents, it has been suggested that microbial metabolic activity depends on the type of organic matter present rather than total abundance (Fukui, et al., 1999; Chapelle, et al., 2002; Hasinger, et al., 2012). Particularly, SRB have been shown to

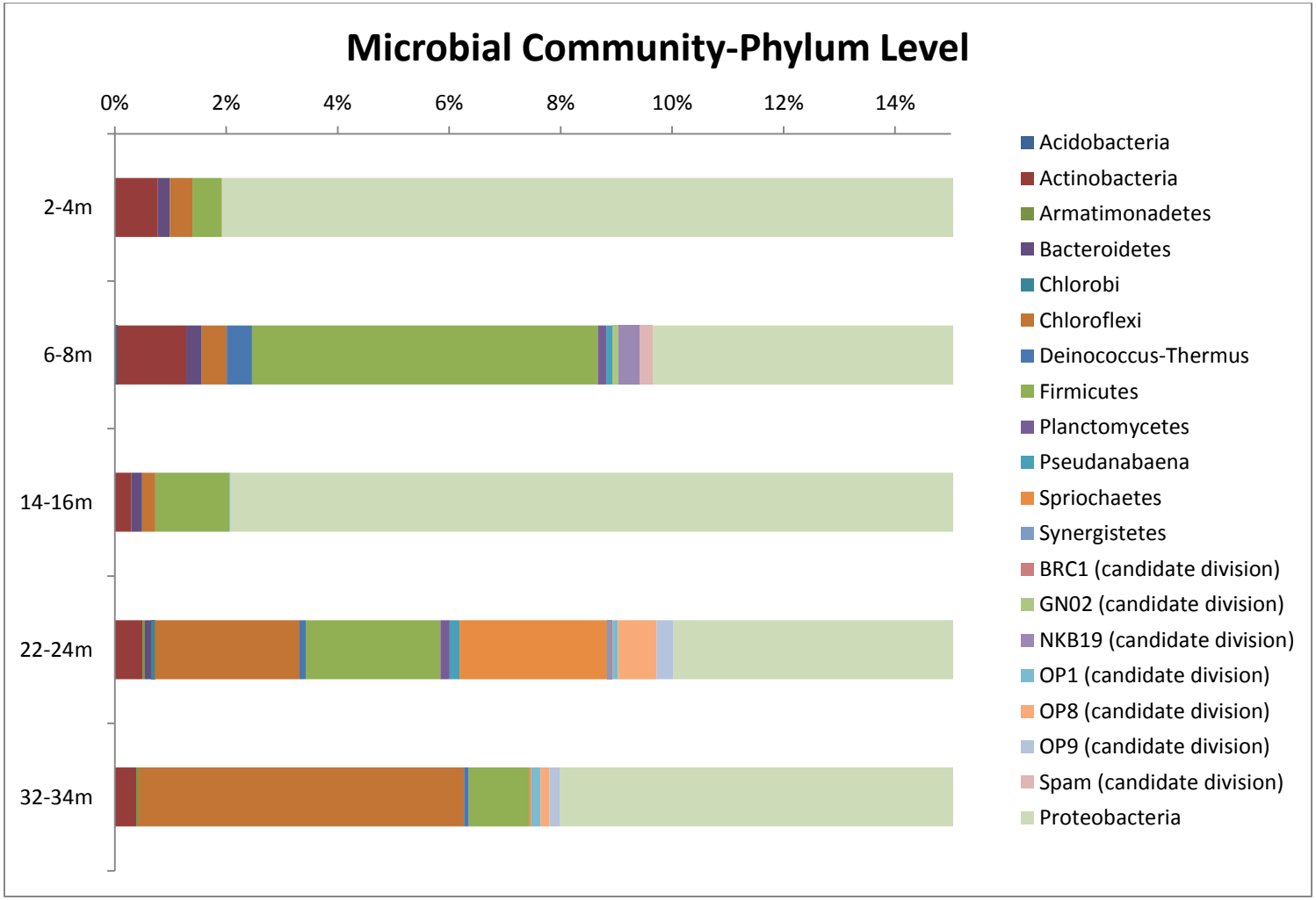

Figure 0.3. CT bacterial community diversity with depth, organized at the Phylum level. Due to the dominance of Proteobacteria (90-98% of total community), the x-axis was magnified to represent 0-14% of community diversity (where anything beyond 14% is Proteobacteria) to highlight the other contributing phyla.

metabolize higher molecular weight compounds (less biologically accessible) quite effectively (Hasinger, et al., 2012). This community difference in CT will favour SO_4^{2-} reduction and generation of H_2S, possibly outcompeting IRB despite the availability of Fe^{3+} down core. Thus, the availability of reactive Fe (Fe^{2+}) will be a determining factor in how much H_2S is present in the system as H_2S will only accumulate after all Fe^{2+} has been exhausted through Fe-sulfide precipitates. Within this deposit, we observed a maximum porewater [Fe^{2+}] of 38.5 µM (2-4 m) and an average [H_2S] of approximately 20 µM generated throughout the CT deposit (excluding 22-24m). Therefore, the concentrations of Fe^{2+} within surface depths of this deposit are currently sufficient to sequestering ambient surficial concentrations of H_2S through Fe-sulfide precipitates (FeS or FeS_2) making H_2S gas release of low concern. However, under maximum conditions where [H_2S] was measured to be 301.5 µM (22-24 m), only 13-26% of H_2S could potentially be sequestered indicating that sequestration may eventually be limited by Fe^{2+}. Outgassing could occur if surficial [H_2S] were to increase (e.g. > 80 µM H_2S) or is H_2S were to migrate upwards (e.g. via diffusion, groundwater flow, anthropogenic alteration of materials) within the deposit (e.g. from 22-24m). Active Fe and S biogeochemical cycling will be an important process within this CT deposit controlling the fate of H_2S. Thus, it is important to understand what the potential microbial dynamics are and how they impact biogeochemical cycling occurring within CT in order to successfully manage and reclaim these types of deposits.

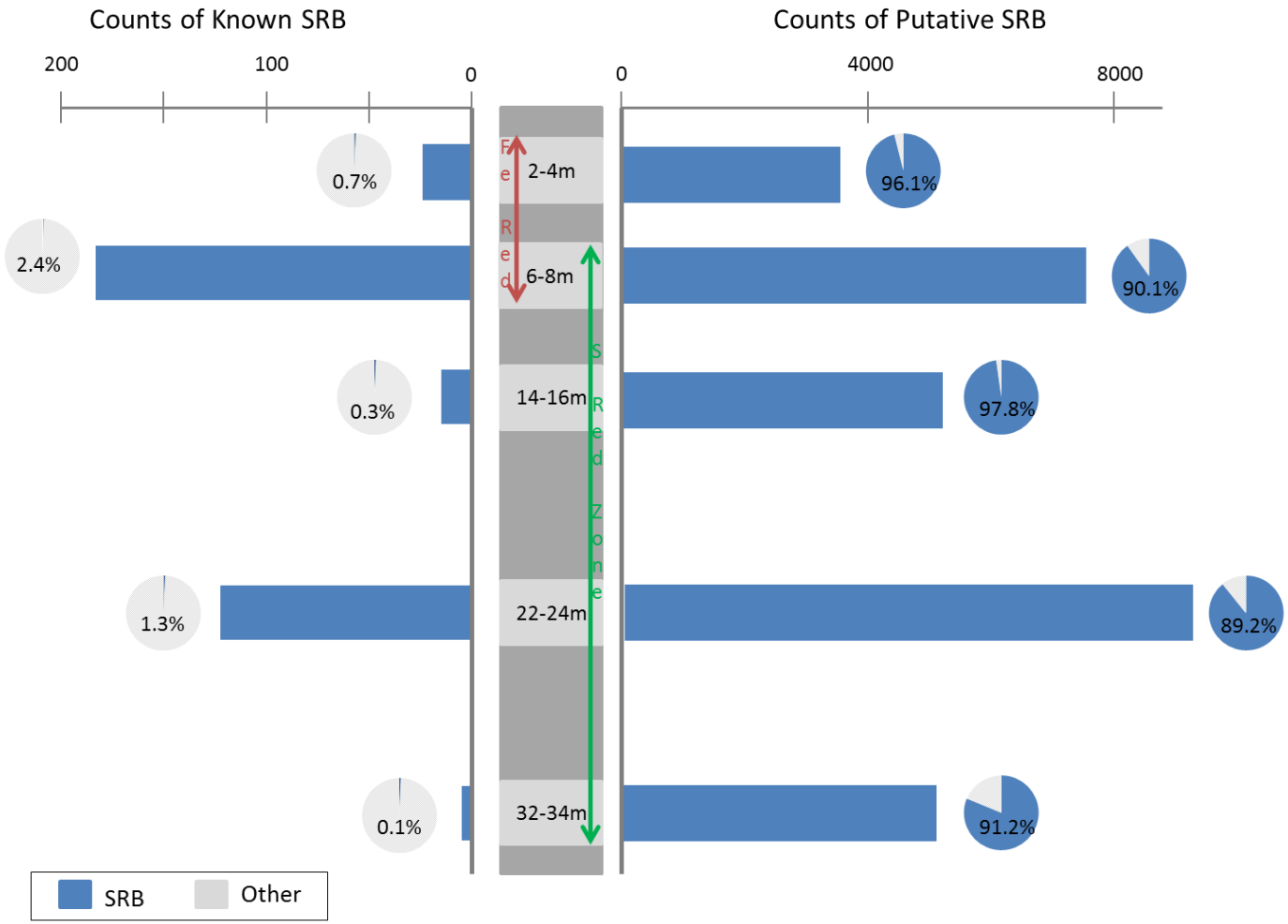

Figure 0.4. Counts (bar charts) and community percentages (pie charts) of known SRB and bacteria putatively capable of SO_4^{2-} reduction across the 5 depths sampled in the CT deposit. Red double headed arrow delineates the observed zone of Fe^{3+} reduction while the green double headed arrow delineates the observed zone of SO_4^{2-} reduction.

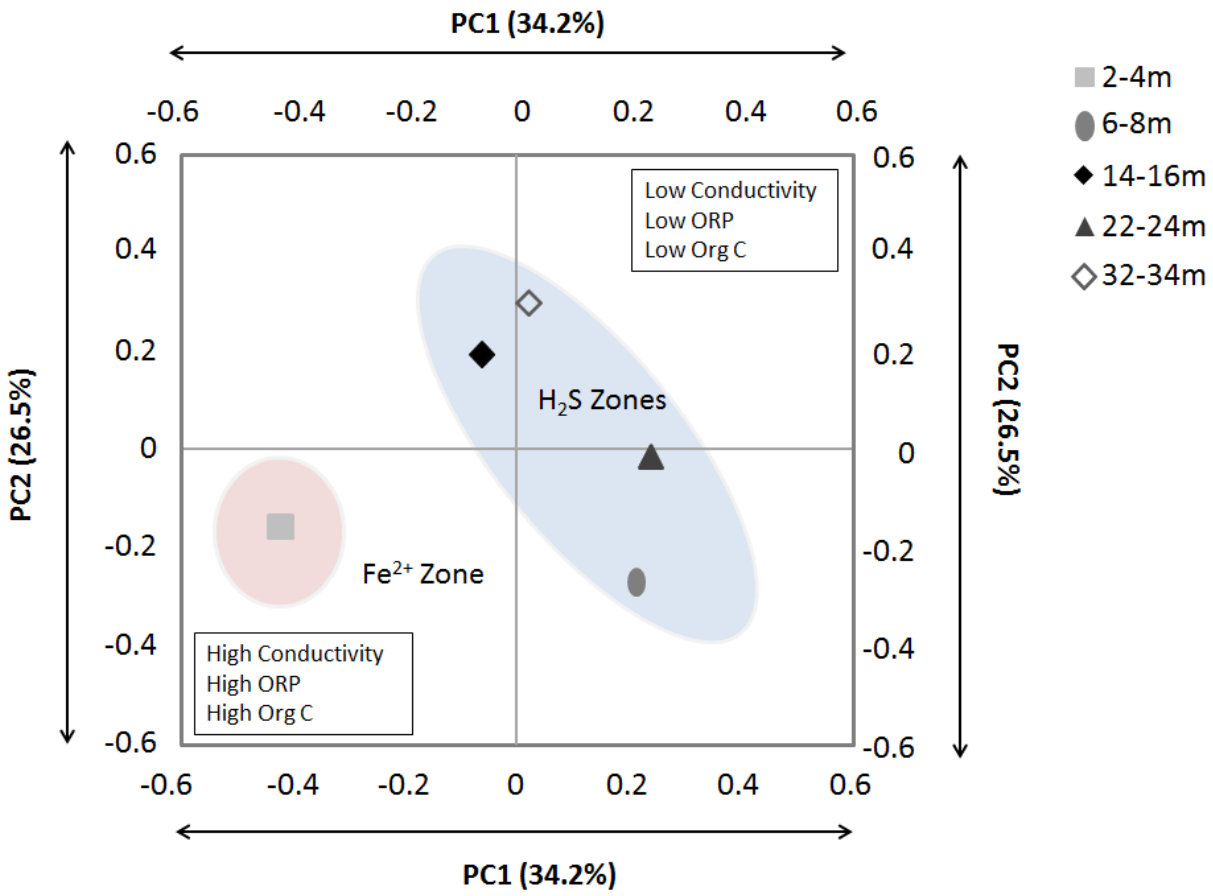

Figure 0.5. Microbial community composition with depth in CT deposit as a function of principal components 1 (PC1) and 2 (PC2). Axis labels refer to the principal components and the total percentage of variance explained by each component. Text boxes infer significantly correlated environmental characteristics associated with microbial community composition: ORP and conductivity (weakly negatively correlated with PC1, $p < 0.1$) and organic C (negatively correlated with PC2, $p < 0.05$). Highlighted clusters correspond with zones of observed porewater [H_2S] and [Fe^{2+}].

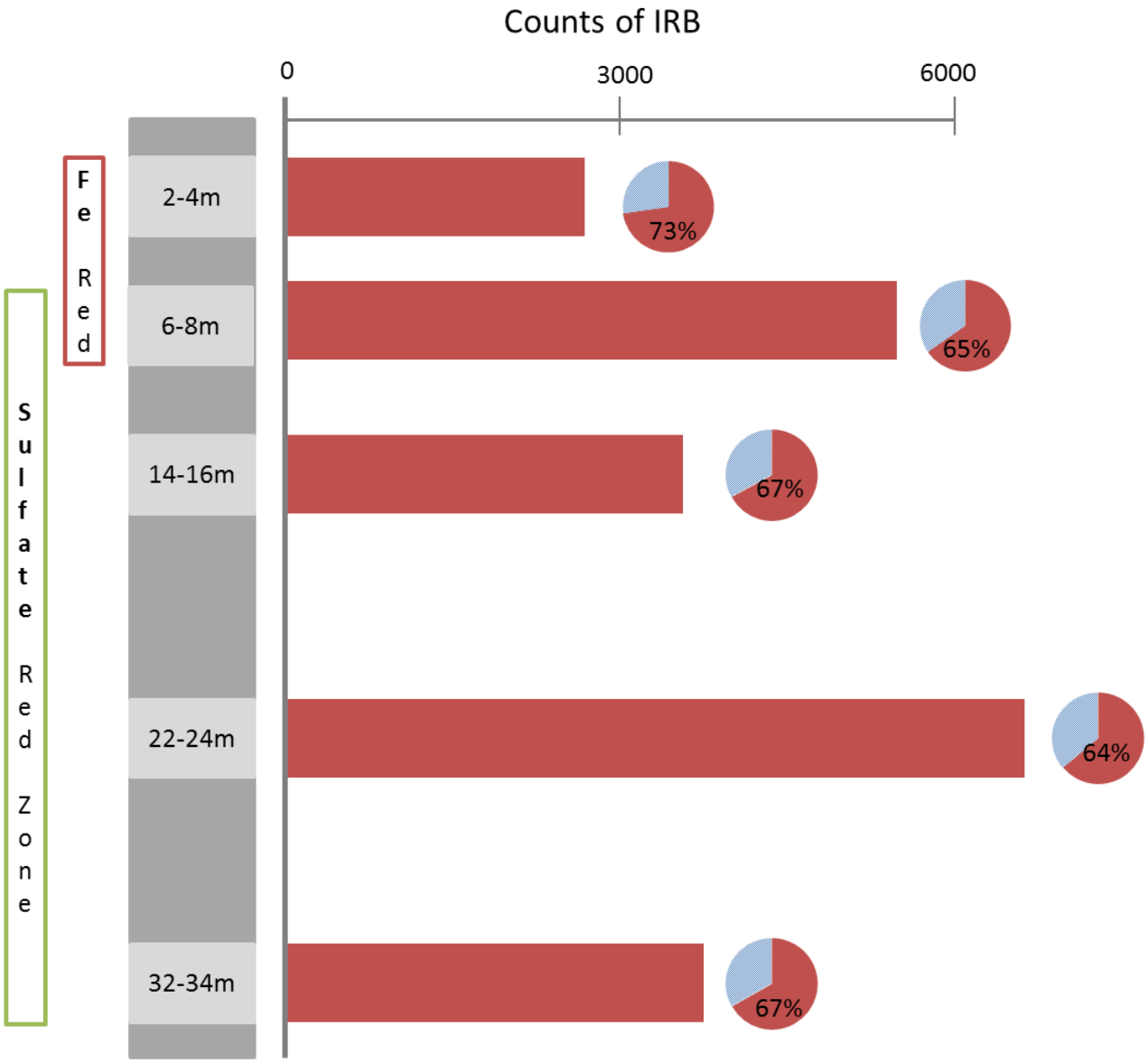

Figure 0.6. Counts and proportions of the total bacterial community putatively capable of Fe^{3+} reduction metabolism in comparison to zones of Fe reduction (red box) and SO42- reduction (green box). Bar charts represent total bacterial counts and pie charts represent the percentage of the total bacterial community. Red portions of bar charts and pie charts (percentage of total community superimposed) represent putative IRB while the grey portion of the pie charts represents the remainder of the bacterial community.

1.0 CONCLUSIONS

The novel results of this thesis establish widespread microbial S biogeochemical cycling to be occurring in an untreated CT deposit within the oil sands, with structurally distinct and highly diverse microbial communities capable of SO_4^{2-}- and Fe^{3+}- reduction as evidenced by depth-dependent porewater Fe and S analyses and characterization of the associated microbial communities though 454 pyrosequencing, functional metabolic enrichments and multivariate UniFrac PCA and clustering analysis. CT porewater [H_2S] was detected extensively throughout the deposit with background levels ranging from 14 – 23 µM and a significantly higher zone occurring at 22-24 m, where 301.5 µM H_2S was detected. CT exhibited concentrations of H_2S higher than those in peatlands but similar to those reported from oil sands tailings and brackish lake sediments. The concentrated H_2S at 22-24 m was not predicted based on the geochemical characterization of CT materials as no major anomalies were observed with depth; pH decreased with depth while temperature increased, ORP and conductivity were variable but generally decreased with depth, Fe-bearing minerals, concentrations of total extractable Fe and percentage of TOC all increased linearly with depth while AVS and AES S components were constant throughout depth. The widespread occurrence of porewater [H_2S], while limited [Fe^{2+}] was confined to the surface depths despite the availability of Fe^{3+} throughout the deposit suggests that labile OC is limiting and that the SRB community may be better able to metabolize more recalcitrant forms of OC, thus outcompeting IRB. Fe^{3+} reduction is active in the shallow subsurface CT zone and the porewater levels of Fe^{2+} are currently sufficient to sequester background concentrations of H_2S (e.g. [H_2S] closest to the surface of the deposit), however, Fe^{2+} concentrations are approximately $1/10^{th}$ those of the maximum H_2S observed at deeper

depth, indicating that that H_2S outgassing is thus possible if H_2S were to migrate upwards in the deposit.

Measureable porewater Fe^{2+} and H_2S, an inverse relationship between H_2S and DOC observed at 22-24 m and the presence of magnetite (mixed-valence $Fe^{2+/3+}$, frequently associated with microbial activity) down core strongly implicate the involvement of microbes in driving S geochemistry within CT. Metagenomic characterization of CT microbial communities identified high diversity with 20 different phyla encountered and 1/3 of these presenting as candidate divisions over the five depths examined. Despite being largely dominated by Proteobacteria, CT demonstrated extensive capacity for SO_4^{2-} and Fe^{3+}- reduction determined through analysis of metagenomic sequencing data in conjunction with environmental enrichments. In fact, over 10 species of known SRB were identified within the bacterial community including *Desulfovibrio* sp., *Desulfuromonas* sp., *Desulfobacter* sp. and *Clostridium* sp., and over 90% of the bacterial community has the capacity for putative SO_4^{2-} reduction. UniFrac multivariate analysis revealed that community structuring within CT is largely driven by DOC concentrations, ORP and conductivity (salinity) and that depths with measurable H_2S clustered together, distinct from the surficial Fe^{2+} producing zone, indicating that SRB and IRB communities are important structural components of the CT microbial community.

Given the emerging evidence of increasing S emissions from the oil sands and the largely methane-focused research conducted in these environments to date, this research has newly identified the need for a better understanding of S dynamics within oil sands waste deposits. Here, we demonstrate that H_2S outgassing is possible but of low concern as the amount of Fe^{2+} being generated within the surficial zone of the CT deposit is sufficient to effectively trap the average concentrations of H_2S being generated at depth. More information is required as to what

factors control the rate of IRB and SRB metabolisms within CT in order to develop better management strategies going forward.

Current reclamation plans for the Kingfisher CT deposit involve the construction of a saltwater fen (in similar fashion to its adjacent neighbour, the Sandhill Fen). However, large inputs of labile organic matter from additions of peat and woody debris may further stimulate an already active and dominant SRB community and further exacerbate H_2S generation. Conversely, labile OC additions could stimulate the IRB community resulting in greater availability of reactive Fe^{2+} to sequester the H_2S generated. Thus, it is important to understand what the potential microbial dynamics are and how they impact biogeochemical cycling occurring within CT in order to successfully manage and reclaim these types of deposits.

2.0 REFERENCES

Algora, C., Grundger, F., Adrian, L., Damm, V., Richnow, H., & Kruger, M. (2013). Geochemistry and microbial populations in sediments of the Northern Baffin Bay, Arctic. *Geomicrobiology Journal, 30,* 690-705.

Auld, R., Myre, M., Mykytczuk, N., Leduc, L., & Merrit, T. (2013). Characterization of the microbial acid mine drainage microbial community using culturing and direct sequencing techniques. *Journal of Microbiological Methods, 93,* 108-115.

Bernier, L. (2007). Sulfur biogeochemistry in a mine tailings lake. *PhD Thesis, McMaster University*.

Bernier, L., & Warren, L. (2005). Microbially driven acidity generation in a tailings lake. *Geobiology, 3,* 115-133.

Bertics, V., & Ziebis, W. (2010). Bioturbation and the role of microniches for sulfate reduction in coastal marine sediments. *Environmental Microbiology, 12*(11), 3022-3034.

Blodau, C., Mayer, B., Peiffer, S. & Moore, T.R. (2007). Support for an anaerobic sulfur cycle in two Canadian peatland soils. *Journal of Geophysical Research, 112,* 1-10.

Borch, T., Kretzschmar, R., Kappler, A., Van Cappellen, P., Ginder-Vogel, M., Voegelin, A., & Campbell, K. (2010). Biogeochemical redox processes and their impact on contaminant dynamics. *Environmental Science and Technology, 44,* 15-23.

Bordenave, S., Kostenko, V., Dutkoski, M., Grigoryan, A., Martinuzzi, R., & Voordouw, G. (2010). Relation between the activity of anaerobic microbial population in oil sands tailings ponds and the sedimentation of tailings. *Chemosphere, 81,* 663-668.

Bouzat, J., Hoostal, M., & Looft, T. (2013). Spatial patterns of bacterial community composition within Lake Erie sediments. *Journal of Great Lakes Research, 39,* 344-351.

Burlage, R., Atlas, R., Stahl, D., Geesey, G., & Sayler, G. (1998). *Techniques in Microbial Ecology.* New York: Oxford University Press.

Bura-Nakic, E., Viollier, E., Jezequel, D., & Thiam, A. C. (2009). Reduced sulfur and iron species in anxoic water column of meromictic crater Lake Pavin (Massif Central, France). *Chemical Geology, 266,* 311-317.

Burton, E., Bush, R., Johnston, S., Sullivan, L., & Keene, A. (2011b). Sulfur biogeochemical cycling and novel Fe-S mineralization pathways in a tidally re-flooded wetland. *Geochimica et Cosmochimica Acta, 75,* 3424-3452 (B).

Burton, E., Bush, R., Sullivan, L., & Mitchell, D. (2007). Reductive transformation of iron and sulfur in schwetmannite-rich accumulations associated with acidified coastal lowlands. *Geochim. Cosmochim. Acta, 71*, 4456-4475.

Burton, E., Johnston, S., & Bush, R. (2011a). Microbial sulfidogenesis in ferrihydrite-rich environments: effects on iron mineraology and arsenic mobility. *Geochimica et Cosmochimica Acta, 75*, 3072-3087 (A).

Canfield, D. (1989). Sulfate reduction and oxic respiration in marine sediments: implications for organic carbon preservation in euxinic enviornments. *Deep Sea Research, 36*(1), 121-138.

Chapelle, F., Bradley, P., Lovely, D., O'Neill, K., & Landmeyer, J. (2002). Rapid evolution of redox processes in a petroleum hydrocarbon-contaminated aquifer. *Groundwater, 40*(4), 353-360.

Cole, J., Wang, Q., Cardenas, E., Fish, J., Chai, B., Farris, R., . . . Tiedje, J. (2009). The ribosomal database project: improved alignments and new tools for rRNA analysis. *Nucleic Acids Res., 37*, 141-145.

Davison, W. (1991). The solubility of iron sulphides in synthetic and natural waters at ambient temperatures. *Aquatic Sciences, 53/4*, 1015-1621.

DeAngelis, K., Silver, W., Thompson, A., & Firestone, M. (2010). Microbial communities acclimate to recurring changes in soil redox potential status. *Environmental Microbiology, 12*(12), 3137-3149.

D'Hondt, S., Jorgensen, B., Miller, D., Batzke, A., Blake, R., Cragg, B., . . . Acosta, J. (2004). Distribution of microbial activities in deep subseafloor sediments. *Science, 306*, 2216-2221.

Dimitriu, P., Prescott, C., Quideau, S., & Grayston, S. (2010). Impact of reclamation of surface-mining boreal forest soils on microbial community composition and function. *Soil Biology and Biochemistry, 42*, 2289-97.

Donisa, C., Steinnes, E., & Mocanu, R. (2008). Combination of different extractants to assess binding forms of some elements in soil profiles. *Communications in Soil Science and Plant Analysis, 39*, 177-186.

Dowd, S., Callaway, T., Wolcott, R., Sun, Y., McKeehan, T., Hagevoort, R., & Edrington, T. (2008). Evaluation of the bacterial diversity in the feces of cattle using 16S rDNA bacterial tag-encoded FLX amplicon pyrosequencing (bTEFAP). *BMC Microbiology, 8*, 125.

Druschel, G., Baker, B., Gihring, T., & Banfield, J. (2004). Acid mine drainage biogeochemistry and Iron Mountain, California. *Geochemical Transactions, 5*(2), 13-32.

Eckford, R., & Fedorak, P. (2002). Chemical and microbiological changes in laboratory incubations of nitrate amendment "sour" produced waters from three western Canadian oil fields. *Journal of Industrial Microbiology and Biotechnology, 29*, 243-254.

Edwards, K., Bond, P., Druschel, G., McGuire, M., Hamers, R., & Banfield, J. (2000). Geochemical and biological aspects of sulfide mineral dissolution: lessons from Iron Mountain, California. *Chemical Geology, 169*, 383-397.

Eiler, A., Langenheder, S., Bertilsson, S., & Tranvik, L. (2003). Heterotrophic bacterial growth efficiency and community strucutre at different natural organic carbon concentrations. *Applied and Environmental Microbiology, 69*(7), 3701-3709.

Elliot, A., & Warren, L. (2013). Seasonal changes in microbial community structure, Fe(III/II)-redox cycling, and trace element geochemistry of pelagic flocs in a circumneutral, remote lake. *Submitted*.

Fortin, D., & Langley, S. (2005). Formation and occurrence of biogenic iron-rich minerals. *Earth-Science Reviews, 72*, 1-19.

Fortin, D., Davis, B., Southam, D., & Beveridge, T. (1995). Biogeochemical phenomena induced by bacteria within sulfidic mine tailings. *Journal of Industrial Microbiology, 14*, 178-185.

Fru, E., Chen, M., Walshe, G., Penner, T., & Weisener, C. (2013). Bioreactor studies predict whole microbial population dynamics in oil sands tailings ponds. *Applied Microbiology Biotechnology, 97*, 3215-3224.

Fukui, M., Harms, G., Rabus, R., Schramm, A., Widdel, F., Zengler, K., . . . Wilkes, H. (1999). Anaerobic degradation of oil hydrocarbons by sulfate-reducing and nitrate-reducing bacterai. *Microbial Ecology of Oil Fields*.

Gieg, L., Davidova, I., Duncan, K., & Suflita, J. (2010). Methanogenesis, sulfate reduction and crude oil biodegradation in hot Alaskan oilfields. *Environmental Microbiology, 12*(11), 3074-3086.

Golby, S., Ceri, H., Gieg, L., Chatterjee, I., Marques, L., & Turner, R. (2012). Evaluation of microbial biofilm communities from an Alberta oil sands tailings pond. *FEMS Microbial Ecology, 79*, 240-250.

Government of Alberta. (2013). *Alberta's Oil Sands*. Retrieved July 15, 2013, from http://www.oilsands.alberta.ca/

Harner, N., Richardson, T., Thompson, K., Best, R., Best, A., & Trevors, J. (2011). Microbial processes in the Athabasca Oil Sands and their potential applications in microbial enhanced oil recovery. *Journal of Industrial Microbiology and Biotechnology, 38*, 1761-1775.

Hasinger, M., Scherr, K., Lundaa, T., Brauer, L., Zach, C., & Loibner, A. (2012). Changes in iso- and n-alkane distribution during biodegradation of crude oil under nitrate and sulphate reducing conditions. *Journal of Biotechnology, 157*, 490-498.

Hazeu, W., Batenburg-van der Vegte, W., Bos, P., van der Pas, R., & Kuenen, J. (1988). The production and utilization of intermediary elemental sulfur during the oxidation of reduced sulfur compounds. *Arch Microbial, 150*, 574-579.

Hsieh, Y., Chung, S., Tsau, Y., & Sue, C. (2002). Analysis of sulfides in the presence of ferric minerals by diffusion methods. *Chemical Geology, 182*, 195-201.

Hugenholtz, P. (2002). Exploring prokaryotic diversity in the genomic era. *Genome Biology, 3*(2).

Keene, A., Johnston, S., Bush, R., Sullivan, L., Burton, E., McElnea, A., . . . Powell, B. (2011). Effects of hyper-enriched reactive Fe on sulfidisation in a tidally inundated acid sulfate soil wetland. *Biogeochemistry, 103*, 263-279.

Kim, B., Oh, H., Kang, H., Park, S., & Chun, J. (2004). Remarkable bacterial diversity in the tidal flat sediment as revealed by 16S rDNA analysis. *J. Microbiol. Biotechnol., 14*(1), 205-211.

Lewis, A. (2010). Review of metal sulphide precipitation. *Hydrometallurgy, 104*, 222-234.

Lozupone, C., & Knight, R. (2005). UniFrac: a new phylogenetic method for comparing microbial communities. *Applied and Environmental Microbiology, 71*(12), 8228-8235.

Lozupone, C., Hamady, M., & Knight, R. (2006). UniFrac - An online tool for comparing microbial community diversity in a phylogenetic context. *BMC Bioinformatics, 7*, 371.

Matthews, J., Shaw, W., Mackinnon, M., & Cuddy, R. (2002). Development of composite tailings technology at Syncrude. *Int. J. Surf. Min. Reclam. Environ., 16*, 24-29.

Meister, P. (2013). Two opposing effects of sulfate reduction on carbonate precipitation in normal marine, hypersaline, and alkaline environments. *Geology, 41*(4), 499-502.

Middelburg, J., & Levin, L. (2009). Coastal hypoxia and sediment biogeochemistry. *Biogeosciences, 6*, 1273-1293.

Mille, G., Almallah, M., Bianchi, M., van Wambeke, F., & Bertrand, J. (1991). Effect of salinity on petroleum biodegradation. *Fresenius Journal of Analytical Chemistry, 339*, 788-791.

Mitterer, R. (2010). 2010. *Earth and Planetary Sciences Letters, 295*, 358-366.

Morse, J., Millero, F., Cornwall, J., & Rickard, D. (1987). The chemistry of hydrogen sulfide and iron sulfide systems in natural waters. *Earth Science Reviews, 24*, 1-42.

Morse, J., Thomson, H., & Finneran, D. (2007). Factors controlling sulfide geochemistry in sub-tropical estuarine and bay sediments. *Aquatic Geochemistry, 13*, 143-156.

Nordstrom, D., Alpers, C., Ptacek, C., & Blowes, D. (2000). Negative pH and extremely acidic mine waters from Iron Mountain, California. *Environmental Science and Technology, 34*, 254-258.

Norlund, K., Southam, G., Tyliszczak, T., Hu, Y., Karunakaran, C., Obst, M., . . . Warren, L. (2009). Microbial architecture of environmental sulfur processes: A novel syntrophic sulfur-metabolizing consortia. *Environmental Science and Technology, 43*, 8781-86.

Nystrand, M., & Osterholm, P. (2013). Metal species in a Boreal river system affected by acid sulfate soils. *Applied Geochemistry, 31*, 133-141.

Oborn, I. (1989). Properties and classification of some acid sulfate soils in Sweden. *Geoderma, 45*, 197-219.

Omoregie, E., Mastalerz, V., de Lange, G., Straub, K., Kappler, A., Roy, H., . . . Boetius, A. (2008). Biogeochemistry and community composition of iron and sulfur precipitating microbial mats at the Chefren Mud Volcano (Nile Deep Sea Fran, Eastern Mediterranean). *Applied and Environmental Microbiology, 74*(10), 3198-3215.

Oremland, R., Marsh, L., & Polcin, S. (1982). Methane production and simulataneous sulfate reduction in anoxic, salt-marsh sediments. *Nature, 296*(5853), 143-145.

Penner, T., & Foght, J. (2010). Mature fine tailings from oil sands processing harbour diverse methanogenic communities. *Canadian Journal for Microbiology, 56*, 459-470.

Peralta, R., Ahn, C., & Gillevet, P. (2013). Characterization of soil bacterial community structure and physicochemical properties in created and natural wetlands. *Science of the Total Environment, 443*, 725-732.

Price, M., Dehal, P., & Arkin, A. (2009). FastTree: computing large minimum evolution trees with profiles instead of a distance matrix. *Mol. Biol. Evol., 26*, 1641-1650.

Proemse, B., Mayer, B., & Fenn, M. (2012). Tracing industrial sulfur contriubtions to atmospheric sulfate deposition in the Athabasca oil sands region, Alberta, Canada. *Applied Geochemistry, 27*, 2425-2434.

Ramos-Padron, E., Bordenave, S., Lin, S., Bhaskar, I., Dong, X., Sensen, C., . . . Gieg, L. (2011). Carbon and sulfur cycling by microbial communities in a gypsum-treated oil sands tailings pond. *Enviornmental Science and Technology, 45*, 439-446.

Reis, M., Barbosa, F., Chartone-Souza, E., & Nascimento, A. (2013). The prokaryotic community of a historically mining-impacted tropical stream sediment is as diverse as that from a pristine stream sediment. *Extremophiles, 17*, 301-309.

Rickard, D., & Luther, G. (2007). Chemistry of iron sulfides. *Chemical Reviews, 107*(2), 514-562.

Roychoudhury, A., Cowan, D., Porter, D., & Valverde, A. (2013). Dissimilatory sulphate reduction in hypersaline coastal pans: an integrated microbialogical and geochemical study. *Geobiology, 14*, 224-233.

Sakai, S., Nakaya, M., Sampei, Y., Dettman, D.L. & Takayasu, K. (2013). Hydrogen sulfide and organic carbon at the sediment-water interface in coastal brackish Lake Nakaumi, SW Japan. *Environ Earth Sci, 68*, 1999-2006.

Salloum, M.J., Dudas, M.J. & Fedorak, P.M. (2002). Microbial reduction of amended sulfate in anaerobic mature fine tailings from oil sand. *Waste Management & Research, 20*, 162-171.

Saidi-Mehrabad, A., He, Z., Tamas, I., Sharp, C., Brady, A., Rochman, F., . . . Dunfield, P. (2013). Methanotrophic bacteria in oilsand tailings ponds of northern Alberta. *International Society for Microbial Ecology, 7*, 908-921.

Sanz-Lazaro, C., Vlademarsen, T., Marin, A., & Holmer, M. (2011). Effect of temperature on biogeochemistry of marine organic-enriched systems: implications in a global warming scenario. *Ecological Applications, 21*(7), 2664-2677.

Schippers, A., & Jorgensen, B. (2001). Biogeochemistry of pyrite and iron sulfide oxidation in marine sediments. *Geochimica et Cosmochimica Acta, 66*(1), 85-92.

Sell, K., & Morse, J. (2006). Dissolved Fe2+ and (sum)H2S behaviour in sediments seasonally overlain by hypoxic-to-anoxic waters as determined by CSV microelectrodes. *Aquatic Geochemistry, 12*, 179-198.

ShimadzuCorporation. (2013). *680 C combusion catalytic oxidation method measurement principles*. Retrieved January 15, 2013, from http://www.shimadzu.com/an/toc/lab/toc-l4.html

Siddique, T., Penner, T., Klassen, J., Nesbo, C., & Foght, J. (2012). Microbial communities involved in methane production from hydrocarbons in oil sands tailings. *Environmental Science and Technology, 46*, 9802-9810.

Stephenson, K. (2012). Seasonal sulfur biogeochemistry of oil sands composite tailings undergoing fen reclamation. *M.Sc. Thesis, McMaster University.*

Suarez-Suarez, A., Lopez-Lopez, A., Tovar-Sanchez, A., Yarza, P., Orfila, A., Terrados, J., . . . Rossello-Mora, R. (2011). Response of sulfate-reducing bacteria to an artifical oil-spill in a coastal marine sediment. *Environmental Microbiology, 13*(6), 1488-1499.

Syncrude Canada Ltd. (2010). *Environment, Health and Safety*. Retrieved September 23, 2011, from http://www.syncrude.ca/users/folder.asp ?FolderID=5717.

Thamdrup, B., Fossing, H., & Jorgensen, B. (1994). Manganese, iron and sulfur cycling in a coastal marine sediment, Aarhus Bay, Denmark. *Geochimica et Cosmochimica Acta, 58*(23), 5115-5129.

Vlademarsen, T., Kristensen, E., & Holmer, M. (2010). Sulfur, carbon and nitrogen cycling in faunated marine sediments impacted by repeated organic enrichment. *Marine Ecology Process Series, 400*, 37-53.

Voordouw, G. (2012). Interaction of oil sands tailings particles with polymers and microbial cells: first steps towards reclamation to soil. *Biopolymers, 99*(4), 257-262.

Wakelin, S., Anand, R., Reith, F., Gregg, A., Nobel, R., Goldfarb, K., . . . Brodie, E. (2012). Bacterial communities associated with a mineral weathering profile at a sulphidic mine tailings dump in arid Western Australia. *FEMS Microbial Ecology, 79*, 298-311.

Wolcott, R., Gontcharova, V., Sun, Y., & Dowd, S. (2009). Evaluation of the bacterial diversity among and within individual venous leg ulcers using bacterial tag-encoded FLX and titanium amplicon pyrosequencing and metagenomic approaches. *BMC Microbiology, 9*, 226-237.

Wu, S., Kuschk, P., Wiessner, A., Muller, J., Saad, R., & Dong, R. (2013). Sulphur transformations in constructed wetlands for wastewater treatment: A review. *Ecological Engineering, 52*, 278-289.

Xie, S., Yang, H., Luo, G., Huang, X., Liu, D., Wang, Y., . . . Xu, R. (2012). Geomicrobial functional groups: a window on the interaction between life and environments. *Chinese Science Bulletin, 57*(1), 2-19.

Zhu, M., Liu, J., Yang, G., Li, T., & Yang, R. (2012). Reactive iron and its buffering capacity towards dissolved sulfide in sediments of Jiaozhou Bay, China. *Marine Environmental Research, 80*, 46-55.

Zopfi, J., Ferdelman, T., & Fossing, H. (2004). Distribution and fate of sulfur intermediates-sulfite, tetrathionate, thiosulfate and elemental sulfur-in marine sediments. *Geological Society of America Special Papers, 379*, 97-116.